Soil Dynamics and Earthquake Engineering 40 (2012) 15–33

Contents lists available at SciVerse ScienceDirect

Soil Dynamics and Earthquake Engineering

journal homepage: www.elsevier.com/locate/soildyn

Rocking response of SDOF systems on shallow improved sand: An experimental study

Ioannis Anastasopoulos *, Rallis Kourkoulis, Fani Gelagoti, Efthymios Papadopoulos

School of Civil Engineering, National Technical University of Athens, Greece

ARTICLE INFO

Article history:
Received 7 August 2011
Received in revised form
3 April 2012
Accepted 18 April 2012

ABSTRACT

Recent studies have highlighted the potential advantages of allowing inelastic foundation response during strong seismic shaking. Such an alternative seismic design philosophy, in which soil failure is used as a "fuse" for the superstructure has recently been proposed, in the form of "*rocking isolation*". Within this context, foundation rocking may be desirable as a means of bounding the inertia forces transmitted onto the superstructure, but incorporates the peril of unacceptable settlements in case of a low static factor of safety FS_v. Hence, to ensure that rocking is materialized through uplifting rather than sinking, an adequately large FS_v is required. Although this is feasible in theory, soil properties are not always well-known in engineering practice. However, since rocking-induced soil yielding is only mobilized within a shallow layer underneath the footing, "shallow soil improvement" is considered as an alternative approach to release the design from the jeopardy of unforeseen inadequate FS_v. For this purpose, this paper studies the rocking response of relatively slender SDOF structures (h/B ratio equals 3 and rocking dominates over sliding), with emphasis on the effectiveness of shallow soil improvement stretching to various depths below the foundation. A series of reduced-scale monotonic and slow-cyclic pushover tests are conducted on SDOF systems lying on a square surface foundation. It is shown that shallow soil improvement may, indeed, be quite effective provided that its depth is equal to the width of the foundation. For lightly-loaded systems, an even shallower soil improvement may also be considered effective, depending on design requirements. The effectiveness of shallow soil improvement is ameliorated with the increase of cyclic rotation amplitude, and with repeating cycles of loading.

1. Introduction

Contemporary earthquake engineering norms aim to alleviate the destruction and avert collapse caused by earthquakes, by allowing ductility-controlled inelastic behavior of the superstructure. Design principles aim at guiding failure to above-ground structural members, prohibiting mobilization of foundation bearing-capacity, uplifting and/or sliding (e.g., [43]). This is typically achieved by imposing over-strength factors and conservative factors of safety against all such possible "failure" modes, which in turn generates substantial ductility requirements on above-ground structural elements. Yet, thanks to the cyclic and kinematic nature of seismic shaking, such mobilization does not necessarily lead to collapse. In fact, recent research suggests that soil compliance and subsequent soil–foundation plastic yielding may be beneficial, and should be considered in analysis and perhaps allowed in design (e.g., [38,40,41,22,18,29]).

In this framework, recent studies have investigated the nonlinear response of soil–foundation–structure systems analytically, by means of sophisticated Winkler-based models [49,34,12,28,1,2,44], advanced macro-element modeling [36,42,31,13,26,10,11,16], and direct numerical methods (finite elements or finite differences) where both the structure and the foundation–soil system are modeled together [48,9,47,25,6]; and experimentally, by means of large-scale cyclic pushover testing [35,15], centrifuge model testing [30,18–20], or reduced-scale cyclic pushover and shaking table testing [39,46,14].

The idea of "rocking isolation" [32] has recently been proposed as an alternative seismic design philosophy in which soil failure is used as a "fuse" for the superstructure. As schematically illustrated in Fig. 1, in contrast to conventional capacity design the foundation is deliberately "under-designed" to promote rocking, thus limiting the inertia forces transmitted onto the superstructure. The potential effectiveness of such a design scheme has been explored analytically [4] and experimentally [3,14] for an idealized RC bridge pier, and for idealized 2-storey RC frame structures [23,24]. It was shown that such "reversal" of capacity design may substantially increase the safety margins against collapse, although it may incur some increased settlement or residual foundation

* Corresponding author. Tel.: +30 2107723383; fax: +30 2107722405.
E-mail address: ianast@civil.ntua.gr (I. Anastasopoulos).

0267-7261/$ - see front matter © 2012 Elsevier Ltd. All rights reserved.
http://dx.doi.org/10.1016/j.soildyn.2012.04.006

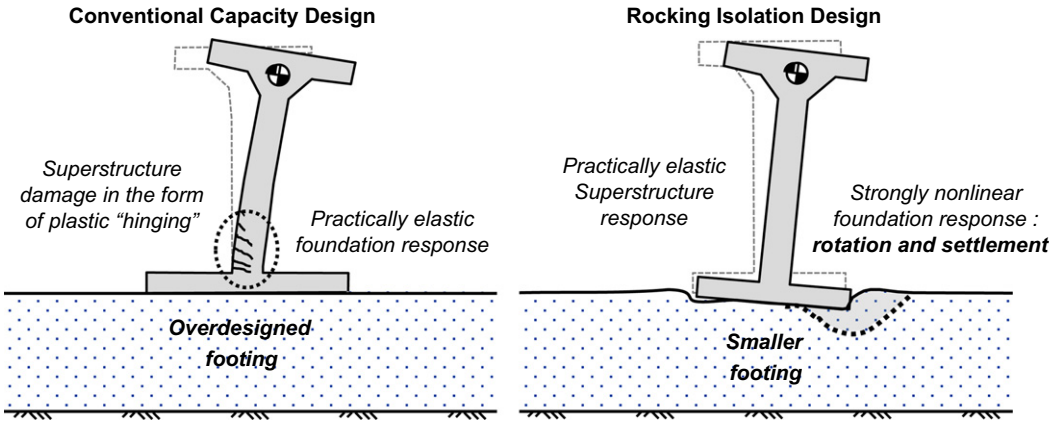

Fig. 1. Conventional capacity design versus rocking isolation. While in a conventionally designed system failure is guided to the superstructure, in a rocking-isolated system the moment capacity of the foundation is fully mobilized to promote rocking and protect the superstructure, at the cost of foundation rotation and settlement.

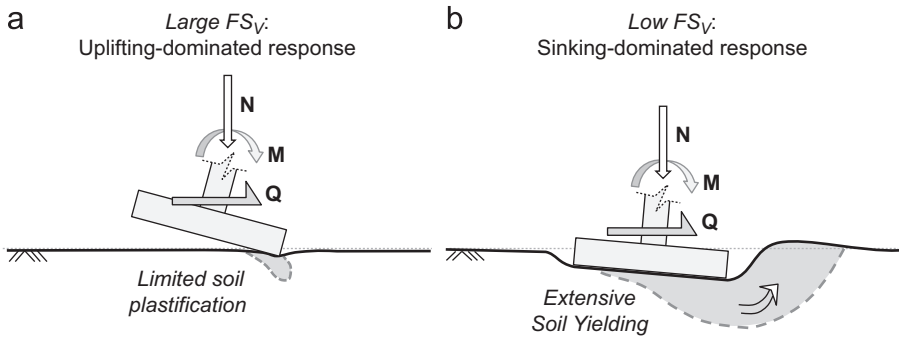

Fig. 2. Rocking response of a surface foundation subjected to combined (M, Q, N) loading, for: (a) relatively large FS_v, where the response is uplifting-dominated and settlement is minimized; and (b) relatively low FS_v, where the bearing capacity failure mechanism is mobilized and the response is sinking-dominated, leading to accumulation of substantial settlement.

rotation. Provided that the safety factor against static (vertical) loads FS_v is maintained adequately large, such kinematically-induced distortion may be maintained within tolerable limits. As sketched in Fig. 2, when FS_v is relatively large, the foundation will respond to strong seismic shaking mainly through uplifting, not accumulating substantial settlement. In stark contrast, in case of lower FS_V excessive soil yielding will take place and the response will be sinking-dominated, leading to substantial accumulation of settlement and permanent rotation, possibly unacceptable for the design. Evidently, ensuring an adequately large FS_V in order to promote uplifting-dominated response greatly depends on the exact soil properties which may not always be accurately known.

In an effort to overcome this obstacle, this paper investigates the potential effectiveness of *shallow* soil improvement, a concept commonly applicable in geotechnical engineering as a means to increase soil strength and reduce settlements. The competence of shallow mitigation stems from the very nature of foundation rocking, which for large FS_V indeed mobilizes only a shallow stress bulb within the soil. Fig. 3 plots the distribution of vertical stresses and the corresponding plastic strains for a lightly loaded ($FS_v=10$) and a heavily loaded ($FS_v=2$) single degree of freedom (SDOF) system subjected to monotonic M–Q loading, computed through nonlinear finite element analysis (as described in [6]). In the first case ($FS_v=10$), the soil below a shallow depth z equal to half the width of the footing ($z/B>0.5$) is not affected by the rocking-induced vertical stresses, with plastic deformation being clearly shallower. In the latter case, the rocking mechanism is deeper, with the vertical stresses being substantially affected at depths $z/B\leq 1$, and plastic deformation evident within a zone of depth $z/B\leq 0.5$.

Motivated by this behaviour, a series of reduced-scale (1 g) monotonic and slow-cyclic pushover tests were conducted in the Laboratory of Soil mechanics of the National Technical University of Athens (NTUA) in order to investigate:

(a) the rocking response of slender SDOF structures under monotonic and slow-cyclic loading, driving them well into their metaplastic regime (i.e., the post-peak behaviour, well beyond their moment capacity), and
(b) the effectiveness of shallow soil improvement stretching to various depths below the foundation. The role of FS_V and of the applied loading protocol is explored parametrically.

It is understandable, that the results produced herein pertain to surface foundations or those shallow embedded; for deeper depths of embedment the results may diverge substantially from the ones shown herein.

2. Problem definition and experimental methodology

A slender $h/B=3$ single degree of freedom (SDOF) system supported on a surface square foundation of width B is studied, considered representative of a relatively slender bridge pier (of prototype dimensions $B=6$ m and $h=18$ m, assuming a scale of 1:40) or a RC column of a frame structure (of prototype dimensions $B=1.5$ m and $h=4.5$ m, assuming a scale of 1:10). Model properties (geometry, mass, stiffness, etc.) were scaled down according to relevant scaling laws [33]. The investigated model configurations are schematically illustrated in Fig. 4. In all cases examined, to focus on foundation performance the superstructure is assumed rigid and elastic. Two superstructure systems are studied, both lying on square foundations: *System A* refers to a lightly loaded

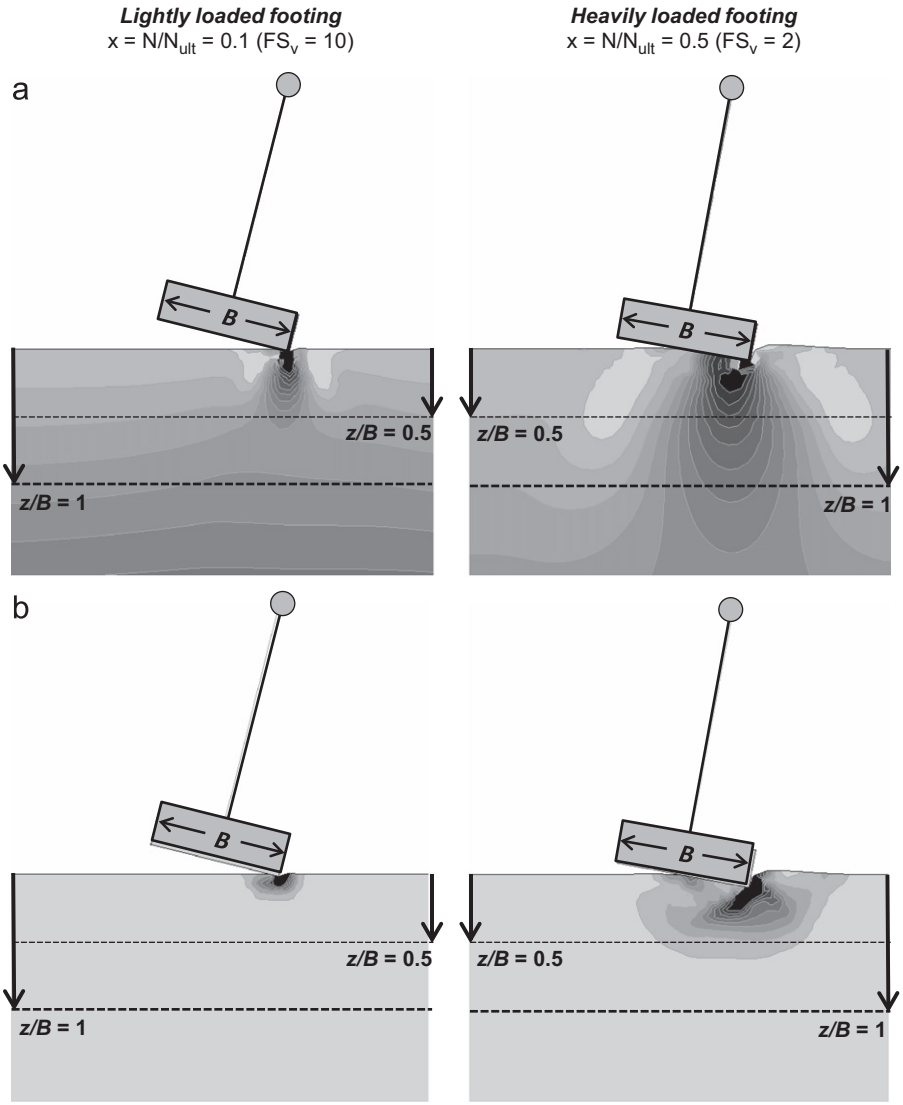

Fig. 3. Illustration of the shallow nature of the rocking mechanism. Numerical simulation of a lightly-loaded ($FS_v = 10$) and a heavily-loaded ($FS_v = 2$) footing : (a) contours of vertical stresses and (b) plastic strain. In the first case, the soil at depth $z/B > 0.5$ is clearly not affected and plastic deformation is even shallower. In the latter case, the rocking mechanism is deeper, with the vertical stresses being substantially affected at depths $z/B \leq 1$, and plastic deformation being contained at $z/B \leq 0.5$.

structure (relatively large FS_v), while *System B* is representative of a heavily loaded structure (relatively low FS_v). The two systems were selected to model distinctly different foundation performance, from uplifting-dominated (*System A*) to sinking-dominated response (*System B*). The two systems were founded in three different soil conditions: (a) dense sand ($D_r = 93\%$), representing the reference case of ideal soil conditions; (b) medium sand ($D_r = 65\%$) for *System A* and loose sand ($D_r = 45\%$) for *System B*, representing poor soil conditions; and (c) soil improvement by means of a shallow "crust" of dense sand, of varying depth $z/B = 0.25$–1. A full width improvement layer was used in the experiments to facilitate preparation of the sand specimen. Nevertheless, in reality the zone of improvement can be of much smaller width. Although the width of the improvement has not been investigated herein, based on numerical analysis results the necessary width of improvement can be of the order of $3B$.

2.1. Foundation–structure modeling

As illustrated in Fig. 5, the foundation–structure model consists of a square $B = 15$ cm aluminum footing, rigidly connected to a pair of rigid steel columns, supporting a rigid aluminum slab positioned at height $h = 45$ cm above the foundation level (to yield the desired $h/B = 3$ slenderness ratio). The superstructure mass (consisting of 1 cm thick steel plates) is installed symmetrically above and below the aluminum slab, so that the center of mass is maintained at the same level. By adding or removing steel plates, the mass of the model (and hence the corresponding FS_v) can be adjusted. Sandpaper was placed underneath the foundation to achieve a realistically rough foundation–soil interface (corresponding to a coefficient of friction $\mu \approx 0.7$). The model was installed inside a rigid 1.6 m long soil container, on top of an adequately deep (concerning the rocking mechanism) $H \approx 3B$ sand stratum, and at an adequately large ($L \approx 5B$) distance from container walls to minimize undesired boundary effects. The model was carefully lowered atop the soil surface by means of four mechanical jacks, enabling its accurate positioning without disturbing the soil surface. Electronic spirit-levels were used to ensure that the foundation was placed horizontally on the soil surface without initial inclination.

2.2. Soil conditions

Dry *Longstone* sand, an industrially produced fine and uniform quartz sand with $D_{50} = 0.15$ mm and uniformity coefficient $C_u = 1.42$, was used in the experiments. Material and strength characteristics

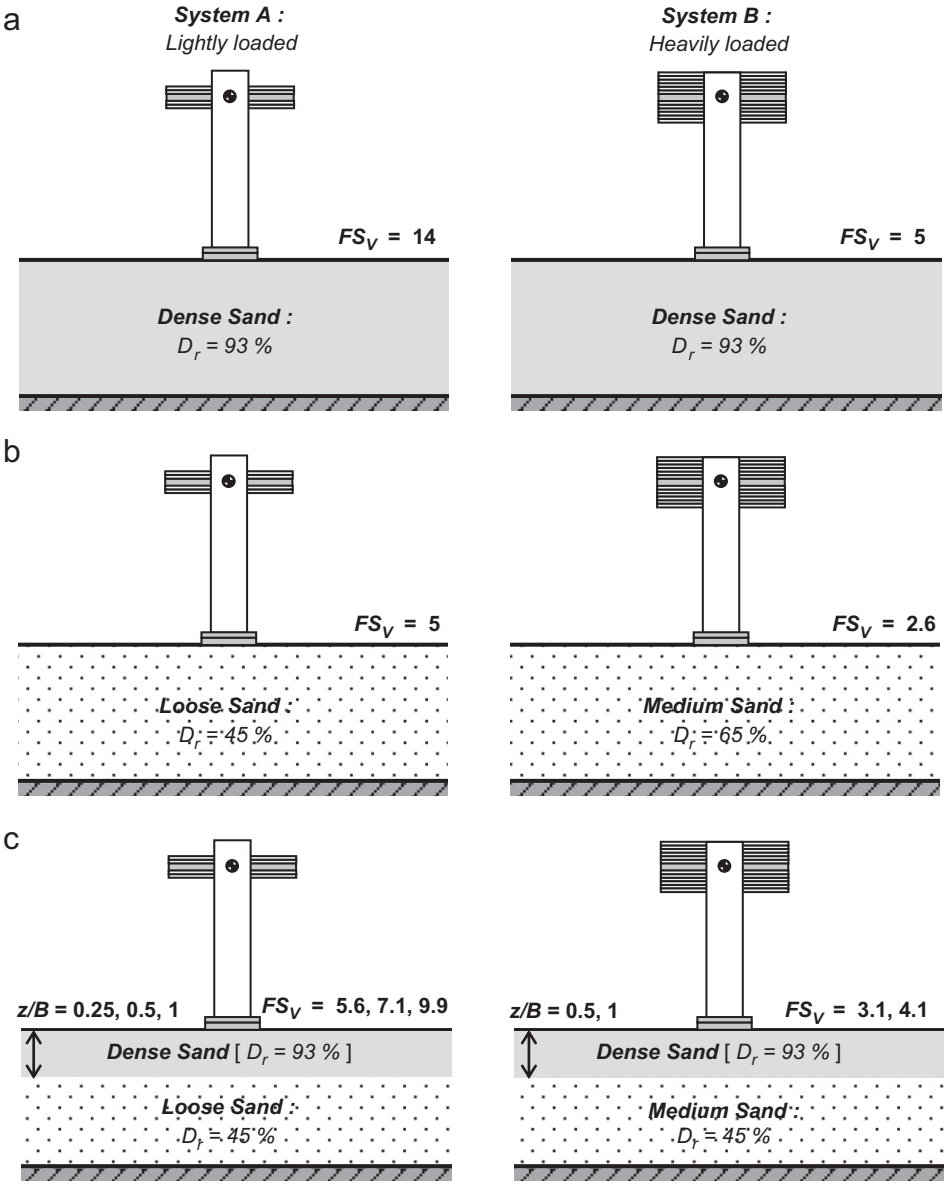

Fig. 4. Schematic illustration of the studied soil-structure systems. Two configurations are investigated, one referring to a lightly loaded system (left), and one referring to a heavily loaded (right) founded on : (a) dense sand, representing the reference case of ideal soil conditions; (b) medium and loose sand, representing poor soil conditions; and (c) soil improvement with a shallow soil crust of dense sand, of varying depth (z/B=0.25 to 1).

of the sand, as derived through laboratory tests, have been documented in Anastastasopoulos et al. [5]. The sand was layered inside the container through an electronically-controlled sand raining system, capable of producing sand specimens of controllable relative density D_r, ensuring repeatability. Adjusting the pluviation height and the raining speed, as well as the aperture of the hopper, enables preparation of soil samples of the desired D_r, from very loose ($D_r \approx 20\%$) to very dense ($D_r > 90\%$). The raining system has been calibrated through a series of pluviation tests, the results of which can be found in Anastastasopoulos et al. [5].

It is well known that reduced-scale experiments cannot reproduce the actual stress field in the supporting soil — a limitation alleviated by centrifuge model testing. Since the strength of the sand is stress-dependent, the significantly lower levels of effective stress in the model result in overestimating φ', which consequently produces larger apparent strength and dilation compared to the prototype. Such shortcomings, commonly referred to as *scale effects*, need to be accounted for when interpreting the results. However, for the problem studied herein, the stresses due to the dead load of the superstructure are prevailing, tending to minimize the adverse role of scale effects. Hence, in order to avoid possible scaling-related misinterpretations, a series of vertical push tests were conducted to measure the bearing capacity of the B=15 cm square foundation for all soil conditions examined. Fig. 6 illustrates the vertical load–settlement (N–w) response for three distinct homogeneous profiles: D_r=93%, representing ideal soil conditions, and medium (D_r=65%) or loose sand (D_r=45%), representing poor soil conditions. It is interesting to note the qualitatively different footing behavior with respect to the soil conditions: the footing on the loose profile displays a strongly hardening response (i.e., the axial load N keeps increasing as the footing accumulates settlement) compared to the footing on dense sand, where the bearing capacity failure (i.e., the instant of the maximum attained vertical load) is indicated by a clear plateau. In the former case the observed increase in the bearing capacity is primarily associated with a considerable increase in the depth of embedment due to the intense settlement, while in the dense the overall footing response is almost unaffected by the minimal initial settlement.

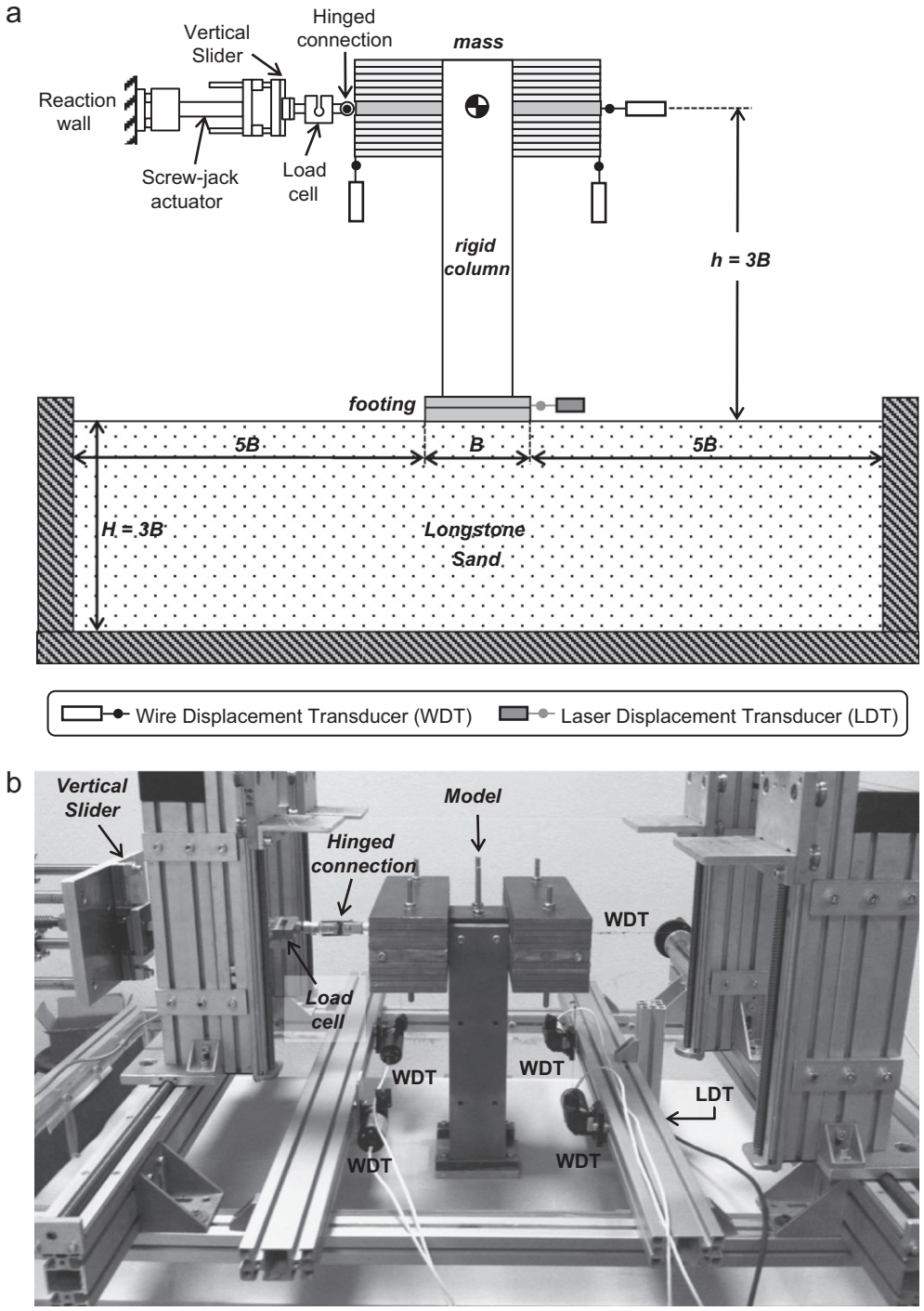

Fig. 5. (a) Experimental setup and instrumentation and (b) photo showing the instrumented model just before a cyclic pushover test.

Based on the results of these tests, which are summarized in Table 1, the mass of the two superstructure models was adjusted to produce the desired FS_v for the reference case of ideal soil conditions (i.e., for dense sand): $FS_v=14$ for the lightly loaded *System A*, and $FS_v=5$ for the heavily loaded *System B*. It should be noted that the determination of the vertical bearing capacity is not always straight forward–especially in loose sand, where the footing settles and the capacity increases continuously. In fact, there are several methods to "define" the vertical bearing capacity, some related to settlement. In this study, the bearing capacity of the foundation N_{ult} is assumed to be reached when the rate of decrease of the tangent vertical stiffness K_v diminishes to zero. This defines the point where the hardening regime initiates, and is believed to be a fairly consistent definition. This yields $N_{ult}=4.83$ kN for dense ($D_r=93\%$) sand, 2.48 kN for medium ($D_r=65\%$) sand, and 1.70 kN for loose ($D_r=45\%$) sand.

2.3. Loading and instrumentation

The desired horizontal displacement is applied directly on the center of mass through a pushover apparatus consisting of a servomotor attached to a screw-jack actuator (Fig. 5). The pushover apparatus is rigidly attached to a reaction wall, while its free end is connected to the foundation–structure model using a vertical slider (materialized through a linear guideway) and a hinged connection (materialized through a pin and clevis attachment) connected in

series, allowing the system to freely settle, slide, and rotate as horizontal displacement is imposed. A load-cell is inserted between the vertical slider and the hinged connection to measure the applied load. Horizontal and vertical displacements were recorded through a combined system of wire and laser transducers, connected to a digital Data Acquisition System.

The nine model configurations of Fig. 4 were subjected to *monotonic* and *slow-cyclic* pushover loading. Previous experimental work by Gajan et al. [18] and [6], suggests that the performance of a rocking foundation subjected to seismic shaking is fairly consistent with the "predictions" of slow cyclic tests. Hence, although rate effects are not taken into account herein, the key conclusions of the present study are considered representative of the response of such systems under seismic shaking. Shaking table test results, which will be presented in a future publication, will further corroborate the findings of the work presented herein.

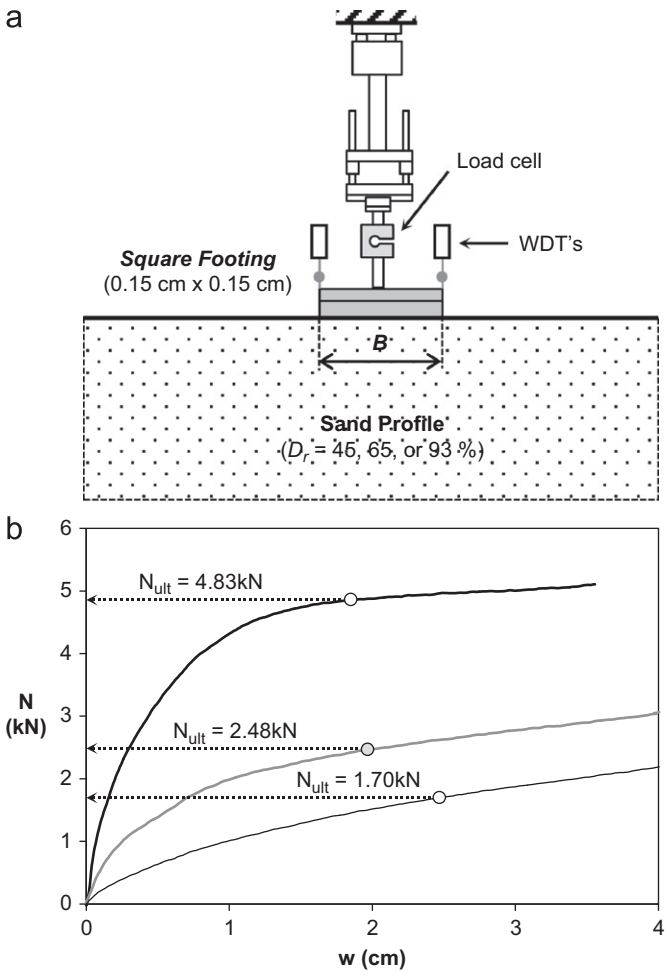

Fig. 6. Monotonic push-down tests on homogeneous sand: (a) experimental setup and (b) vertical load–settlement (N–w) response for D_r =45, 65, and 93%.

In the course of investigating the effect of the displacement amplitude and the sequence of lateral loading on the behavior of the foundation, two different cyclic loading protocols were implemented. As shown in Fig. 7, the primary Type 1 load protocol consists of 14 cycles of increasing displacement δ/δ_R (where δ_R=7.5 cm is the toppling displacement of the equivalent rigid block) ranging from 0.025 to 0.55 (i.e., from 2 mm to 40 mm). Type 2 consists of 31 cycles, divided into: (i) 10 cycles of 0.05 (i.e., 4 mm) amplitude, (ii) 10 cycles of 0.10 (i.e., 8 mm) amplitude, (iii) 5 cycles of 0.20 (i.e., 16 mm), (iv) 3 cycles of 0.30 (i.e., 24 mm), and (v) 3 cycles of 0.55 (i.e., 40 mm amplitude). In this latter case, the displacement was imposed in 5 consecutive load packets. Type 1 protocol should be rather treated as a set of pulses of different amplitudes than as representative of a specific earthquake type, mainly aiming to identify the effect of loading amplitude. Type 2 on the other hand, may be considered as a series of idealized earthquake events (ranging from small amplitude to rather destructive), while it also serves as a means to quantify the effect of number of cycles.

3. Uplifting versus sinking response: The necessity for soil improvement

The first set of experiments aimed at pointing out the profound dissimilarities in the rocking behavior of SDOF systems which are incurred by the differences in FS_v. To this end, the lightly-loaded *System A* and the heavily-loaded *System B*, were subjected to monotonic and slow-cyclic pushover loading lying on homogeneous soil layers (as shown in Figs. 4(a) and 4(b)) of dense sand (D_r=93%), representing ideal soil conditions, and medium (D_r=65%) or loose sand (D_r=45%), representing poor soil conditions.

Figs. 8 and 9 summarize the performance of the two systems subjected to monotonic and cyclic pushover loading, in terms of moment–rotation and settlement–rotation response. Following Gajan and Kutter [19], to allow for more direct and insightful comparisons, moment and rotation are normalized to the overturning moment M_R=mg$B$/2 and toppling rotation ϑ_R=B/2h of the corresponding rigid block (M_R=0.026 and 0.074 kNm for *System A* and *System B*, respectively; ϑ_R=0.167 rad for both), while settlement is normalized to the width B (=15 cm) of the footing. The overturning moment M of the system is directly calculated by the measured load value F multiplied by the lever arm h (i.e., $M=F\times h$). It is clarified that the observed moment capacity degradation (for ϑ/ϑ_R values greater than 0.2) is due to second order phenomena (P–δ effects) that become more prominent as the slenderness of the system increases.

The experimental results have been validated against the failure envelopes of Butterfield and Gottardi [8] in [14]. It was shown, that the lateral capacity of the foundation compares well

Table 1
Summary of measured bearing capacity of the B=15 cm square foundation, for homogeneous (dense, medium, and loose sand) and two-layered soil profiles (dense sand crust on top of medium or dense sand).

	System A			***System B***		
	Configuration	**N_{ult} (kN)**	**FS_v**	**Configuration**	**N_{ult} (kN)**	**FS_v**
Ideal soil conditions	Dense sand (D_r=93%)	4.83	14.1	Dense sand (D_r=93%)	4.83	4.9
Poor soil conditions	Loose sand (D_r=45%)	1.70	5.0	Medium sand (D_r=65%)	2.48	2.6
Soil improvement	z/B=0.25 on top of loose sand	1.95	5.6	z/B=0.25 on top of medium sand	3.03	3.1
	z/B=0.5 on top of loose sand	2.45	7.1	z/B=0.5 on top of medium sand	3.73	3.7
	z/B=1 on top of loose sand	3.40	9.9	z/B=1 on top of medium sand	3.96	4.1

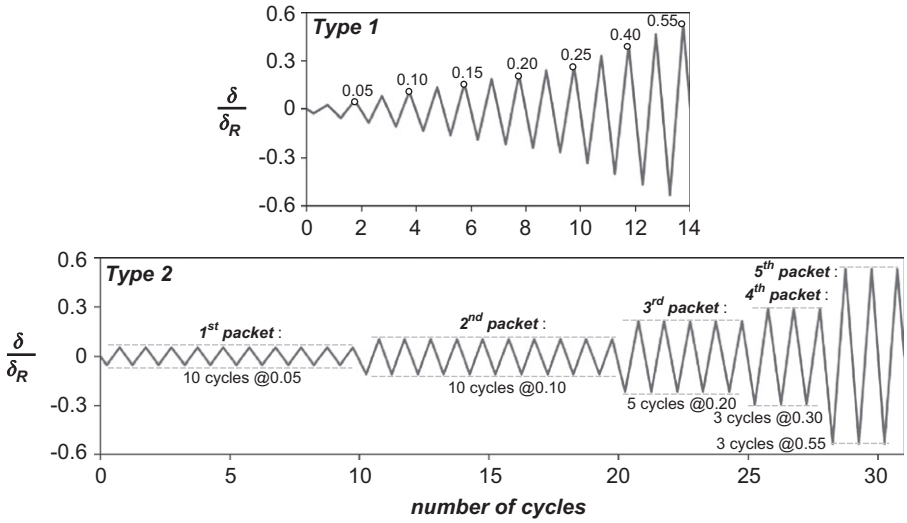

Fig. 7. The two displacement protocols used for cyclic loading tests, normalized to the toppling displacement δ_R of the equivalent rigid block (for the $B=15$ cm foundation used in the tests, $\delta_R=7.5$ cm).

with the published closed-form expression, especially if scale effects are thoroughly taken into account in the estimation of the effective friction angle φ', which is a function of confining stress [7].

In terms of monotonic pushover response (Figs. 8(a) and 9(a)), the performance of the two systems does not seem to deviate from any rational intuitive expectation: the systems with large FS_v (founded on dense sand) demonstrate higher normalized moment capacity and overturning rotation than their low FS_v counterparts (founded on medium or loose sand). While in the first case (dense sand) the response is clearly uplifting-dominated, in the latter case (medium or loose sand) more soil yielding takes place, distorting the equilibrium of the two systems and accelerating their toppling at lower rotation angles. The differences become more notable in terms of settlement–rotation response. Observe that the heavily-loaded *System B* on medium sand, having $FS_v=2.6$, exhibits an invariably sinking-dominated response, toppling at $\vartheta/\vartheta_R<0.6$. In marked contrast, all other configurations with $FS_v>5$ clearly exhibit uplifting-dominated response, with toppling taking place at substantially higher rotational amplitudes: for the lightly-loaded *System A* on dense sand ($FS_v=14$), overturning is observed at $\vartheta/\vartheta_R\approx 1$. Thus, it would be reasonable to conclude that a critical value of FS_v exists, somewhere between 2.6 and 5, beneath which uplifting is impeded-an observation which is in accord with centrifuge model test results [20]. On the other hand, for lower rotational amplitudes all foundations are subjected to settlement, with the exception of the $FS_v=14$ system where uplifting is observed even for very low imposed rotation ($\vartheta/\vartheta_R<0.05$).

When it comes to cyclic loading, for the lightly-loaded *System A* (Fig. 8(b)), the considerable difference in FS_v (14 for dense sand, as opposed to 5 for loose sand) is luminously reflected on the measured moment-rotation loops. While for $FS_v=5$ the loops demonstrate an oval shape, with $FS_v=14$ they become more *S-shaped*. In this latter case, when the system is subjected to large rotation the concentration of stresses underneath the edge of the footing produces localized soil bulging, which results in loss of full contact between the foundation and the soil, therefore reducing the effective rocking stiffness of the foundation during unloading and producing this characteristic *S-shaped* loops. The $FS_V=14$ results compare qualitatively well with experiments on similar, but larger ($B=0.5$ m), square footings performed at PWRI ($h/B\approx 3$ oscillator with $FS_{V,H}\approx 30$ and $h/B\approx 2$ specimen with $FS_{V,L}\approx 14$) [17]. As expected, the PWRI test loops on $h/B\approx 3$ specimens are more S-shaped than those produced here since those tests have been conducted at an impressive $FS_{V,H}\approx 30$, where foundation uplifting was prominent. On the other hand, for the case of $FS_{V,L}\approx 14$ uplifting was naturally more evident in our tests which were conducted on more slender specimens.

For the heavily-loaded *System B* (Fig. 9(b)), the differences in terms of moment-rotation response are not that pronounced. In both cases (i.e., for dense and medium sand), the produced loops are oval-shaped. What is common to both systems (lightly-loaded and heavily-loaded) is the observed *overstrength* during cyclic loading of the respective low FS_v configurations. While in case of the $FS_v=14$ model, the monotonic dimensionless moment-rotation curve clearly "envelopes" the loops of the slow-cyclic tests, the latter tend to overly exceed it when FS_v is reduced. This phenomenon, also observed by Gajan and Kutter [19], may be attributed to the gradual increase in the bearing capacity of shallow foundations (of relatively low FS_V) with accumulating settlement, which may in turn act as a "non-intended" embedment (Fig. 5), or even to sand densification underneath the foundation due to multiple loading cycles. Another possible explanation of the observed overstrength is related to the constructive contribution of second order P–δ effects, as shown by [37]. Quite strikingly, for the lower $FS_v=2.6$ system (Fig. 8(b)), the overstrength keeps increasing with imposed loading cycles, ultimately exceeding the monotonic capacity by a factor of almost 2, while for the larger $FS_v=5$ model, the number of cycles does not seem to have an equally significant effect and the overstrength does not exceed 1.25.

But the most important difference lies in the settlement that is accumulated during cyclic loading. For both systems, the settlement increases substantially with the reduction of FS_v: subjected to the Type 1 loading protocol, the heavily-loaded *System B* on medium sand ($FS_v=2.6$) accumulates almost two times larger settlement compared to the same system on dense sand. Interestingly, even for a remarkably large $FS_v=14$ (*System A* on dense sand) a limited, yet non-negligible, rocking-induced settlement is observed. Nevertheless, it should be noted that this observation is totally in accord with UC Davis centrifuge model test results [19].

As evidenced by the results presented so far, foundation rocking may be desirable (to limit the inertia forces transmitted

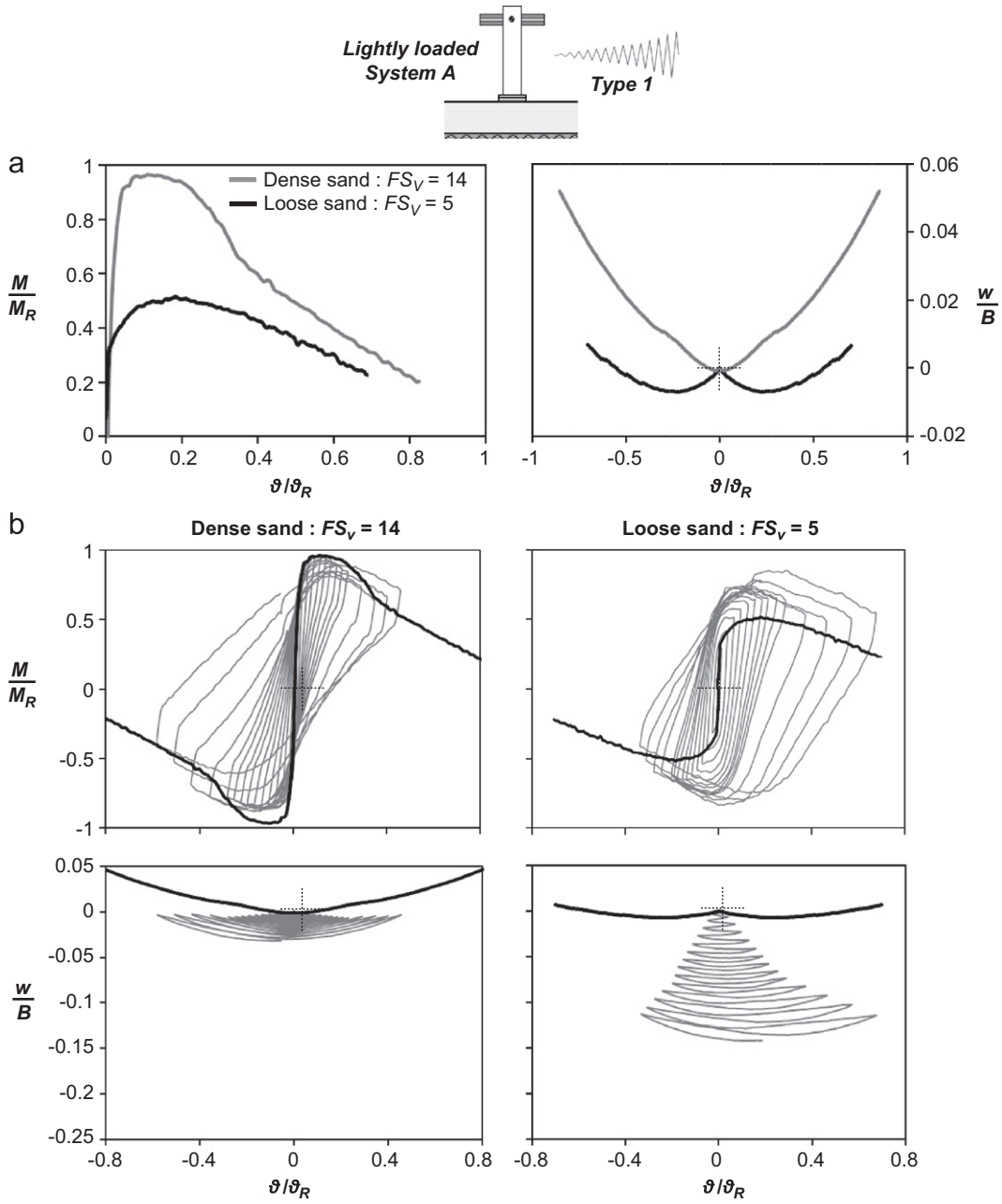

Fig. 8. Moment–rotation and settlement–rotation response of the Lightly loaded *System A* on dense and loose sand subjected to displacement-controlled: (a) monotonic loading and (b) cyclic loading (with Type 1 protocol). Moment and rotation are normalized to the overturning moment M_R (M_R=0.026 kNm) and toppling rotation θ_R of the equivalent rigid block ($\vartheta = h/2B$=0.167 rad); settlement is normalized to the width B of the footing.

onto the superstructure) but incorporates the peril of unacceptable settlements in case of low FS_v. Thus, for foundation rocking to materialize through uplifting rather than settlement, an adequately large FS_v has to be ensured. Plausibly however, the intrinsic uncertainties in the exact estimation of in-situ soil properties would also hinder the exact assessment of FS_v, practically limiting the applicability of rocking-isolation in seismic design. Still though, rocking-induced soil yielding (which is responsible for the accumulation of settlement) is only mobilized within a shallow layer underneath the footing. Driven by this mechanism, the following sections attempt to propose an alternative towards overcoming the limitations of rocking-isolation by investigating the effectiveness of "shallow soil improvement", i.e., the replacement of a shallow soil layer with soil of known (better) properties. If successfully applied, this method would release the design from the jeopardy produced by an unforeseen inadequate safety factor (due to possible over-estimation of the soil properties).

4. Effectiveness of shallow soil improvement for the lightly-loaded structure

As previously discussed, in the case of the lightly-loaded *System A*, the depth z/B of the shallow soil crust of dense sand (D_r=93%) was varied parametrically from 0.25 to 1 (see also Fig. 4(c)). The lowest case of z/B=0.25 was proven to be less effective, and hence, the results are presented for z/B=0.5 and 1. Foundation performance in dense sand is considered as the ideal case, constituting the upper bound that should ideally be approached by applying shallow soil improvement.

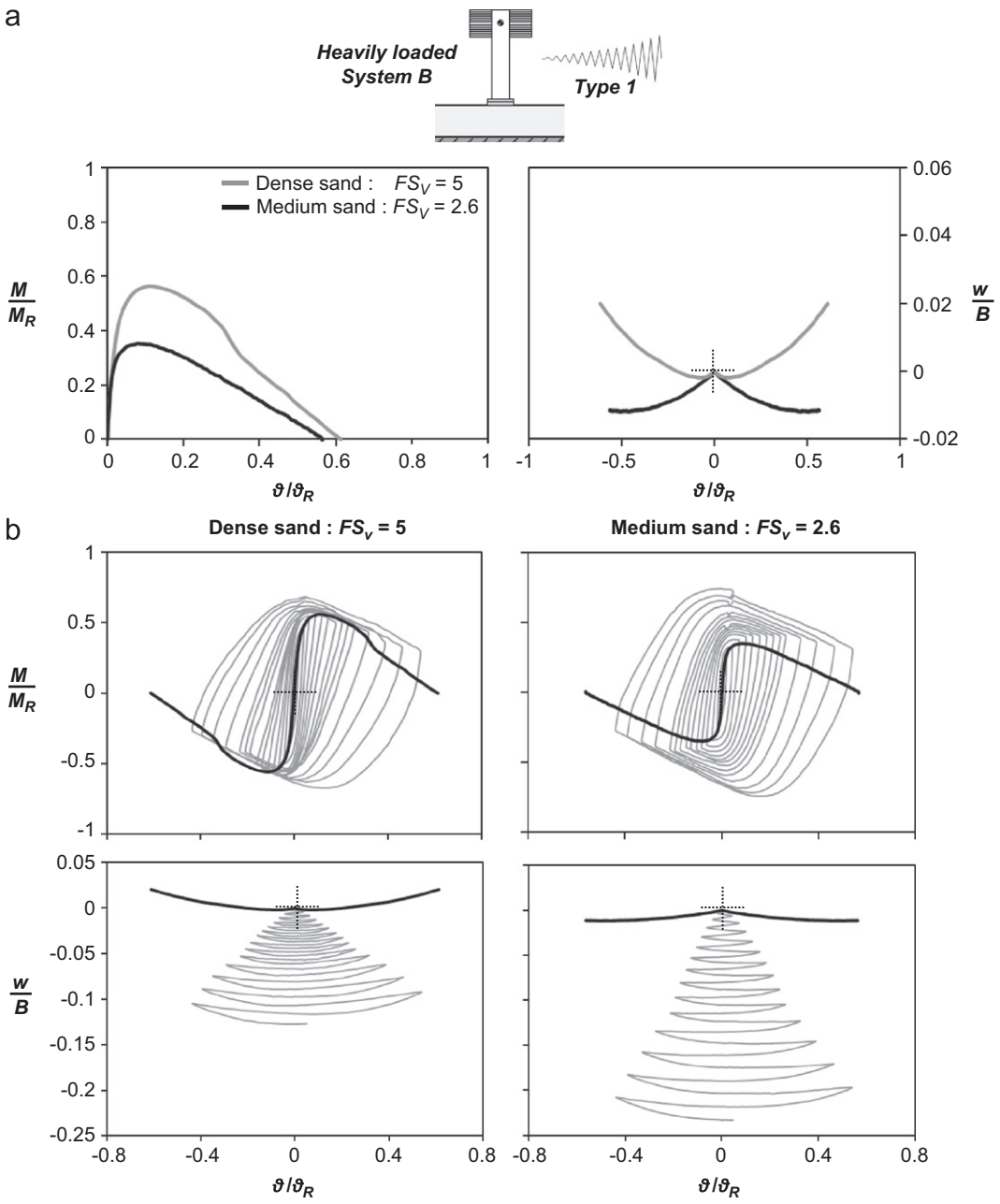

Fig. 9. Moment–rotation and settlement–rotation response of the Heavily loaded System B on dense and medium sand subjected to displacement-controlled (a) monotonic loading and (b) cyclic loading (with Type 1 protocol). Moment and rotation are normalized to the overturning moment M_R (M_R=0.075 kNm) and toppling rotation θ_R of the equivalent rigid block (θ_R=h/2B=0.167 rad); settlement is normalized to the width B of the footing.

4.1. Monotonic loading

The effectiveness of shallow soil improvement for the lightly-loaded *System A* subjected to monotonic pushover loading is summarized in Fig. 10. In terms of moment–rotation response (Fig. 10(a)), as it would be expected the moment capacity of the foundation rises with the increase of the depth z/B of soil improvement, as a result of progressive enhancement of soil strength. As evidenced from the slope of the descending branch, a similar trend is observed for the toppling rotation: the larger the depth of soil improvement, the greater the required ϑ/ϑ_R for toppling. The increase of the thickness of the dense sand crust reduces the extent of soil plastification, which tends to be restricted within the layer of increased strength (not "penetrating" to the underlying loose sand layer of lower strength). Hence, at large rotations the behavior of the model lying on the layered soil profile is almost identical to the upper bound case of ideal soil conditions (i.e., model founded on a homogenous layer of dense sand). Recall that for the lightly-loaded superstructure, the homogenous dense sand profile yields FS_V=14, implying very limited compliance, approaching the response of a rigid block rocking on rigid base (the toppling ϑ/ϑ_R tends to 1).

The differences are more conspicuous in terms of settlement–rotation response (Fig. 10(b)). The grey shaded areas represent the rotation range where the response is governed by sinking. Evidently, with the increase of soil improvement depth z/B, uplifting is promoted for a wider rotation range. Indeed, while for the unimproved soil (loose sand), the footing settles up to ϑ/ϑ_R=0.54, for a z/B=0.5 improved crust the sinking threshold drops considerably to ϑ/ϑ_R=0.24, and to a mere ϑ/ϑ_R=0.04 when z/B=1, becoming almost identical with the ideal case of homogenous dense sand. Moving outside the shaded areas to larger

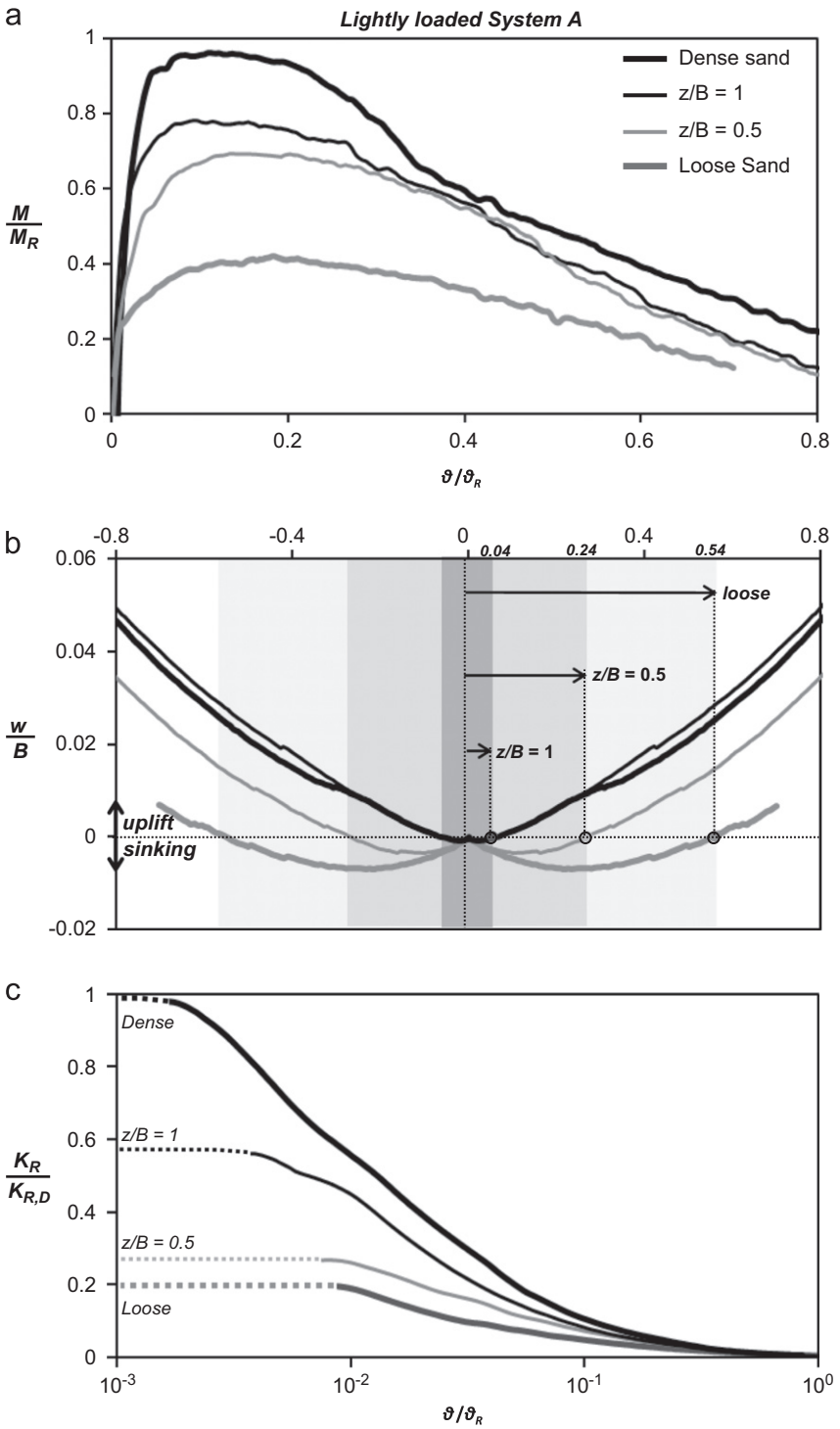

Fig. 10. Effectiveness of soil improvement for the lightly loaded *system A* subjected to monotonic loading. Comparative assessment in terms of: (a) normalized moment-rotation (M_R=0.026 kNm, θ =0.167 rad) and (b) settlement–rotation response (highlighting sinking-dominated response for each case) ; (c) ratio of rocking stiffness K_R to the initial (i.e., small strain) rocking stiffness K_R,D for the ideal case of dense sand ($K_{R,D}$=10.5 kNm/rad).

rotations, where uplifting governs the response, the performance of the models lying on shallow soil improvement is practically identical to the upper-bound case of dense sand (their moment–rotation curves are almost parallel). This enhancement of the effectiveness of shallow soil improvement with the increase of imposed rotation is quite straightforward to explain. Initially (for small ϑ/ϑ_R), the foundation is in full contact with the supporting soil, generating a deeper stress bulb, and hence being affected by the underlying loose sand layer. When uplifting commences, the effective width of the foundation (i.e., the foundation breadth that maintains contact with the soil) is drastically decreased, thus reducing the depth of the generated stress bulb. In effect, the rocking-induced stresses are "confined" to a smaller depth, consequently enhancing the effectiveness of the dense sand crust. In other words, for $\vartheta/\vartheta_R > 0.24$ the foundation on the mitigated soil profiles responds as if founded on homogenous dense sand. Observe that although the z/B=1 curve practically coincides with dense sand up to $\vartheta/\vartheta_R \approx 0.3$, it tends to override it for larger

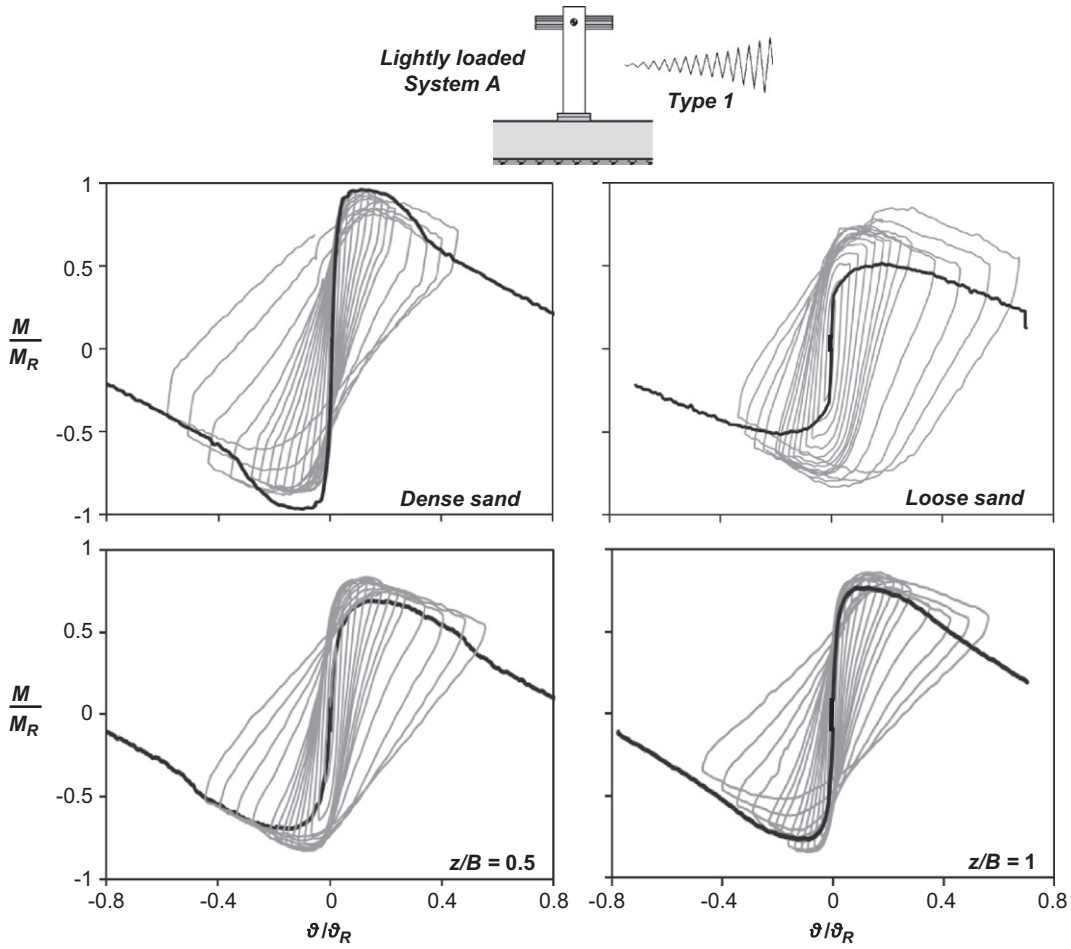

Fig. 11. Effectiveness of soil improvement for the lightly loaded *system A* subjected to cyclic loading (Type 1 protocol). Comparative assessment in terms of moment–rotation response (M_R=0.026 kNm, θ_R=0.167 rad).

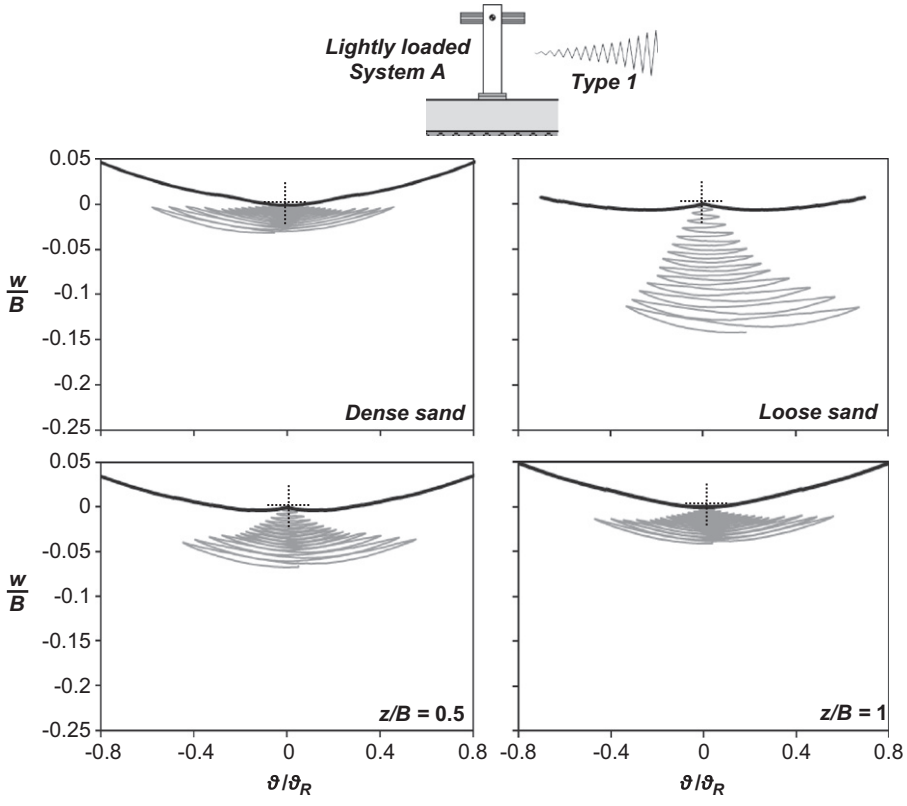

Fig. 12. Effectiveness of soil improvement for the lightly loaded *system A* subjected to cyclic loading (Type 1 protocol). Comparative assessment in terms of settlement–rotation response (B=0.15 m, θ_R=0.167 rad).

rotations. Apparently, this is due to a measurement error (in the dense sand experiment) and should be ignored.

Fig. 10(c) compares the evolution with ϑ/ϑ_R of the rotational stiffness K_R normalized to the initial (i.e., small strain) rocking stiffness $K_{R,D}$ for the ideal case of dense sand. As measured, K_R and $K_{R,D}$ refer to the specific $h/B=3$ SDOF systems, incorporating the coupled rotational stiffness produced under simultaneous M–Q loading. Note that the exact measurement of the initial (i.e., at very small strains) rotational stiffness cannot be achieved (as it would require much higher sensor accuracy, not available today). Therefore a rational approximate extension of the measured K_R is plotted with dotted lines for very small θ/θ_R. For small rotation amplitudes (for a given confining stress, i.e., for the same superstructure dead load), the rotational stiffness is proportional to the small strain shear modulus G_o [21], which increases with the relative density D_r of the sand [45,27]. Hence, the measured increase of the rotational stiffness of the foundation with the increase of the depth z/B of the dense sand crust is quite

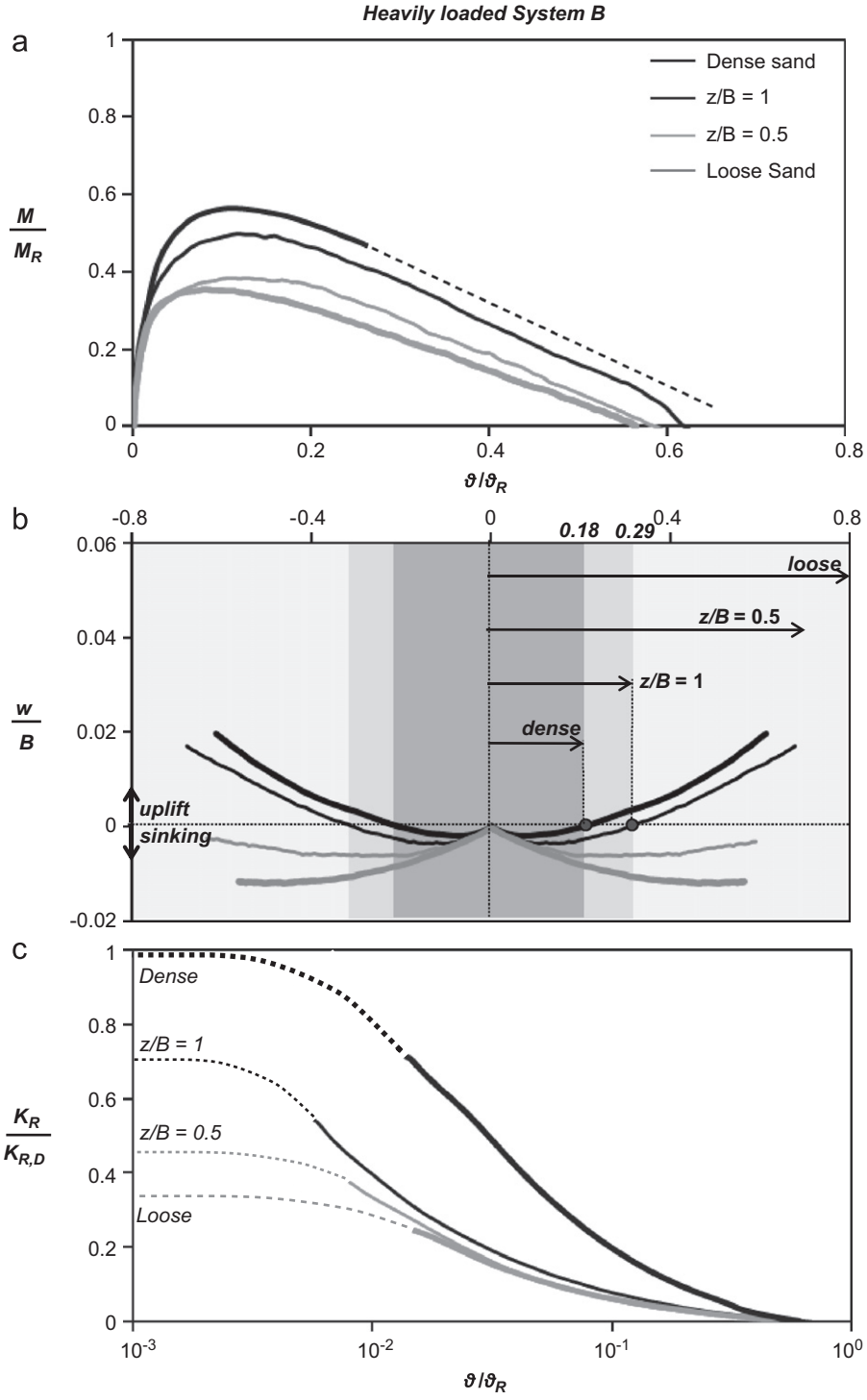

Fig. 13. Effectiveness of soil improvement for the heavily loaded system B subjected to monotonic loading. Comparative assessment in terms of : (a) normalized moment–rotation (M_R=0.075 kNm, θ_R=0.167 rad), and (b) settlement–rotation response (highlighting sinking-dominated response for each case); (c) ratio of rocking stiffness K_R to the initial (i.e., small strain) rocking stiffness *KR,D* for the ideal case of dense sand ($K_{R,D}$ =23.4 kNm/rad).

reasonable. While in the case of the shallower $z/B=0.5$ crust the stiffness almost coincides with the lower bound loose sand case, for $z/B=1$ a substantial increase of $K_R/K_{R,D}$ is observed.

4.2. Cyclic loading

Typical cyclic pushover test results are presented in Figs. 11 and 12, focusing on Type 1 loading protocol. In terms of moment-rotation response (Fig. 11), it is quite evident that as the depth z/B of soil improvement increases, the loops tend to transform from oval-shaped (resembling loose sand) to the *S*-shaped loops of the ideal case of dense sand. Interestingly, contrary to monotonic, in cyclic loading all systems tend to display very similar moment capacity. In effect, this reveals that the overstrength increases with decreasing FS_v, an observation which is consistent with the findings of the previous sections regarding the tests on homogenous soil.

Fig. 12 summarizes the effectiveness of the shallow soil crust in terms of settlement–rotation response, for the same loading protocol. The differences are now quite striking. Even with the "shallow" $z/B=0.5$ soil improvement, the response is palpably superior to that on loose sand. Although the accumulated settlement is still larger than what is observed in the ideal case of dense sand, the effectiveness of the shallow dense sand crust is undeniable. A deeper $z/B=1$ soil improvement is even more effective, leading to practically the same settlement accumulation with the upper bound case of dense sand.

Hence, it can be argued that a $z/B=1$ dense sand crust is enough to achieve practically the same performance with the ideal case of dense sand. A shallower improvement may also be considered as effective, depending on the desired performance and design requirements.

5. Effectiveness of shallow soil improvement for the heavily-loaded structure

As for the previous case, results are presented for $z/B=0.5$ and 1 for the heavily-loaded *System B*. Foundation performance in dense sand is considered as the ideal case.

5.1. Monotonic loading

Fig. 13 outlines the effectiveness of shallow soil improvement for the heavily-loaded *System B* subjected to monotonic pushover testing, applying the same loading protocol (Type 1). As for the previously discussed lightly-loaded *System A*, shallow soil improvement leads to an increase of the foundation moment capacity (Fig. 13(a)). Interestingly, while for the light *System A* the shallow $z/B=0.5$ soil improvement was quite effective, leading to almost 80% enhancement of the moment capacity compared to loose sand (Fig. 10(a)), for the heavily-loaded foundation its effect is barely noticeable both in terms of moment capacity and toppling rotation. On the other hand, the deeper $z/B=1$ soil improvement is still effective, tending to approach the ideal dense sand response. A major difference between the two systems lies in the level of

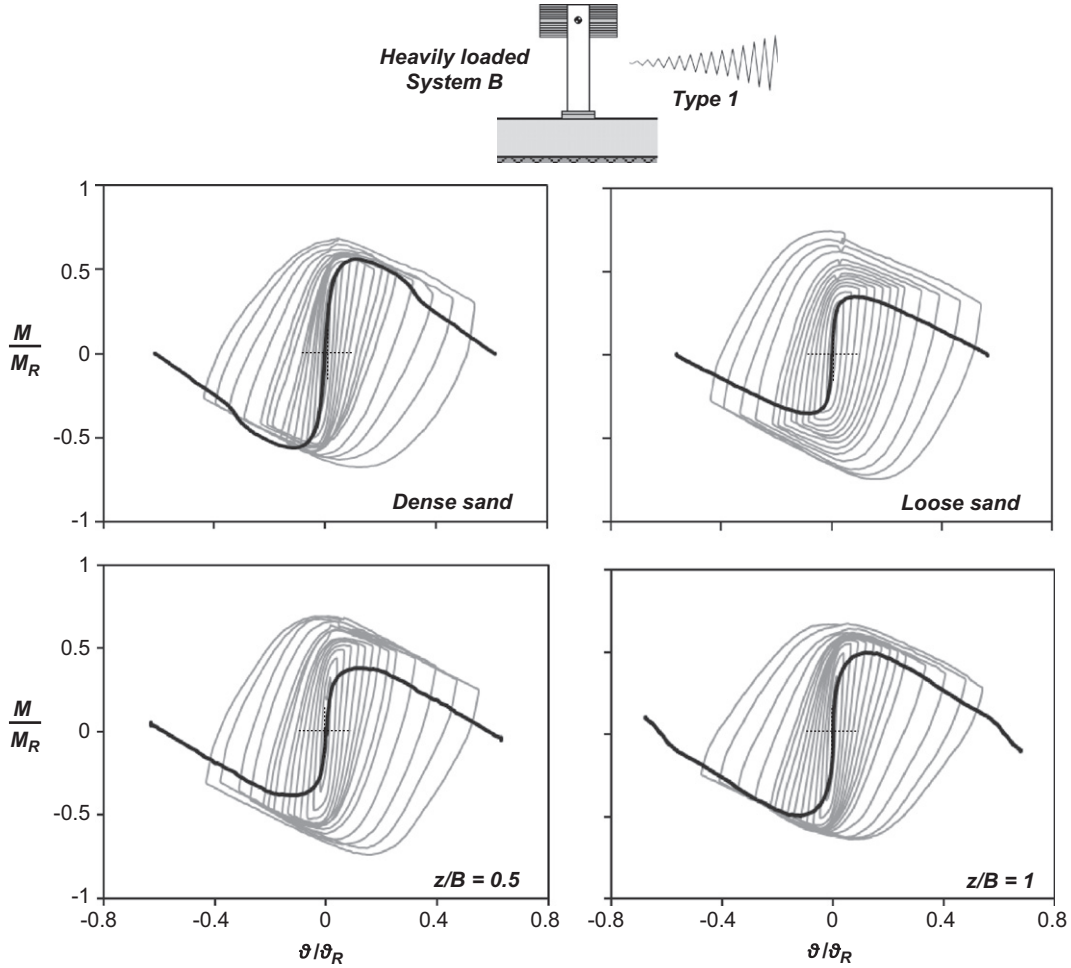

Fig. 14. Effectiveness of soil improvement for the heavily loaded system B subjected to cyclic loading (Type 1 protocol). Comparative assessment in terms of moment-rotation response ($M_R=0.075$ kNm, $\theta_R=0.167$ rad).

achieved FS_v: while for the lightly-loaded *System A*, a rather large $FS_v=14$ was attained for ideal soil conditions (i.e., in dense sand), the corresponding "ideal" FS_v does not exceed 5 for the heavily-loaded *System B*. As a result, even under ideal soil conditions the response of the heavily-loaded foundation cannot be uplifting-dominated, but is rather accompanied by mobilization of bearing capacity and substantial soil plastification. With limited uplifting taking place, the effective width of the foundation is not reduced as much, and the rocking-induced stress bulb tends to "penetrate" deeper, in a manner qualitatively similar to the numerical example of Fig. 3(b).

In terms of settlement–rotation response (Fig. 13(b)) the main conclusions drawn for the lightly-loaded *System A* still hold true, with the main difference being the critical improvement depth (i.e., the z/B necessary to promote uplifting). For relatively small rotation amplitudes, $\theta/\theta_R<0.1$, the foundation settles under any soil conditions (even for the ideal case of dense sand). As a result, the behavior of the models on improved sand is almost identical to that on loose sand, revealing an almost negligible effect of soil improvement. While in loose sand ($FS_v=2.6$) foundation response is sinking-dominated throughout the entire rotation range, a shift towards uplifting is observed at $\vartheta/\vartheta_R=0.18$ in dense sand. In case of the deep $z/B=1$ dense sand crust, the uplifting region initiates for slightly larger $\vartheta/\vartheta_R=0.29$. The shallow $z/B=0.5$ soil improvement cannot be considered effective, exhibiting sinking-dominated response throughout the entire range of ϑ/ϑ_R.

The above mechanisms are also reflected in the measured rocking stiffness (Fig. 13(c). Although shallow soil improvement has a qualitatively similar effect to the previously discussed lightly-loaded *System A* (the rocking stiffness increases with z/B), its effectiveness is remarkably reduced. In fact, it cannot be argued that the shallow $z/B=0.5$ dense sand crust has any measurable effect on the rocking stiffness. Even for the deeper $z/B=1$ soil improvement, the differences from loose sand are not that evident.

5.2. Cyclic loading

The same conclusions are drawn examining the results of slow-cyclic pushover tests. The effectiveness of shallow soil improvement is portrayed in Fig. 14 in terms of moment-rotation response (for the same loading protocol: Type 1). As for the lightly-loaded *System A*, thanks to the observed cyclic overstrength (which, apparently, increases with the reduction of FS_v), the cyclic moment capacity is almost the same for all soil profiles examined, especially after application of the larger amplitudes of loading when the overstrength has been fully mobilized. In contrast to the lightly-loaded *System A*, with FS_v ranging from 2.6 (in loose sand) to 5 (in dense sand), the moment-rotation loops are always oval-shaped.

The effectiveness of shallow soil improvement in terms of settlement–rotation response is summarized in Fig. 15. In accord with the trends observed during monotonic pushover testing, the

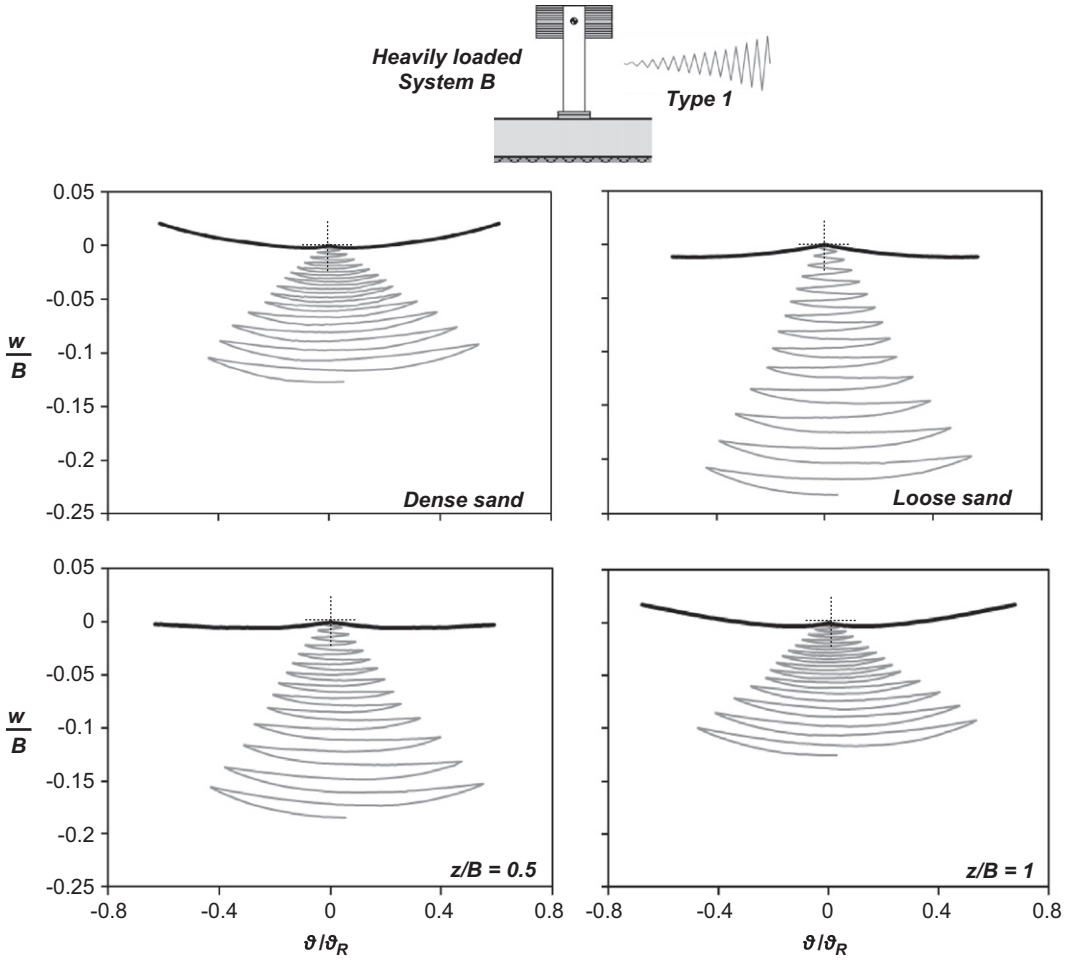

Fig. 15. Effectiveness of soil improvement for the heavily loaded system B subjected to cyclic loading (Type 1 protocol). Comparative assessment in terms of settlement–rotation response ($B=0.15$ m, $\theta_R=0.167$ rad).

response of the foundation is always sinking-dominated. As a result, even in the ideal case of dense sand the foundation accumulates a considerable amount of settlement during each loading cycle. In contrast to the lightly-loaded *System A*, the accumulated settlement (at the end of the Type 1 loading sequence) is now reduced by merely 30% for relatively shallow $z/B=0.5$ improvement. In order to achieve a significant reduction, a deeper $z/B=1$ dense sand crust is required.

6. Performance assessment for multiple loading cycles

So far, the effectiveness of shallow soil improvement has been explored focusing on Type 1 loading protocol, which contains 14 cycles of increasing normalized displacement δ/δ_R, ranging from 0.025 to 0.55 (i.e., from 2 to 40 mm). To assess the performance of shallow soil improvement when the foundation-structure system is subjected to multiple loading cycles, focus will now be on Type 2 loading protocol, which consists of 31 cycles, divided into five consecutive packets of increasing displacement amplitude (from 4 mm to 40 mm).

Fig. 16 portrays the evolution of normalized settlement w/B with respect to the normalized imposed rotation ϑ/ϑ_R for both systems subjected to the multi-cycle Type 2 loading protocol. Although the ultimate displacement amplitude (and hence, rotation) is the same with that of Type 1 loading protocol, in this case strong amplitude cycles are preceded by a multitude of loading cycles of considerably lower imposed displacement (load packets 1 through 4). This loading protocol is expected to contain the dual effect of increasing the accumulated settlement and affecting the soil density underneath the footing.

Indeed, as illustrated in Fig. 16(a), for the lightly-loaded *System A* (with $FS_v=14$ when founded on dense sand), the effectiveness of soil improvement is quite impressive, even for this admittedly severe loading protocol. Even with a shallow $z/B=0.5$ improvement, the accumulated settlement (after 31 loading cycles) is reduced by a factor of almost 3 compared to the loose sand. While for the models on loose sand, settlement is accumulated for all levels of imposed rotation, the models on dense sand and improved soil tend to accumulate settlement only during the initial smaller-amplitude cycles. Further increase of the thickness of the dense sand crust to $z/B=1$ does not seem to reduce the

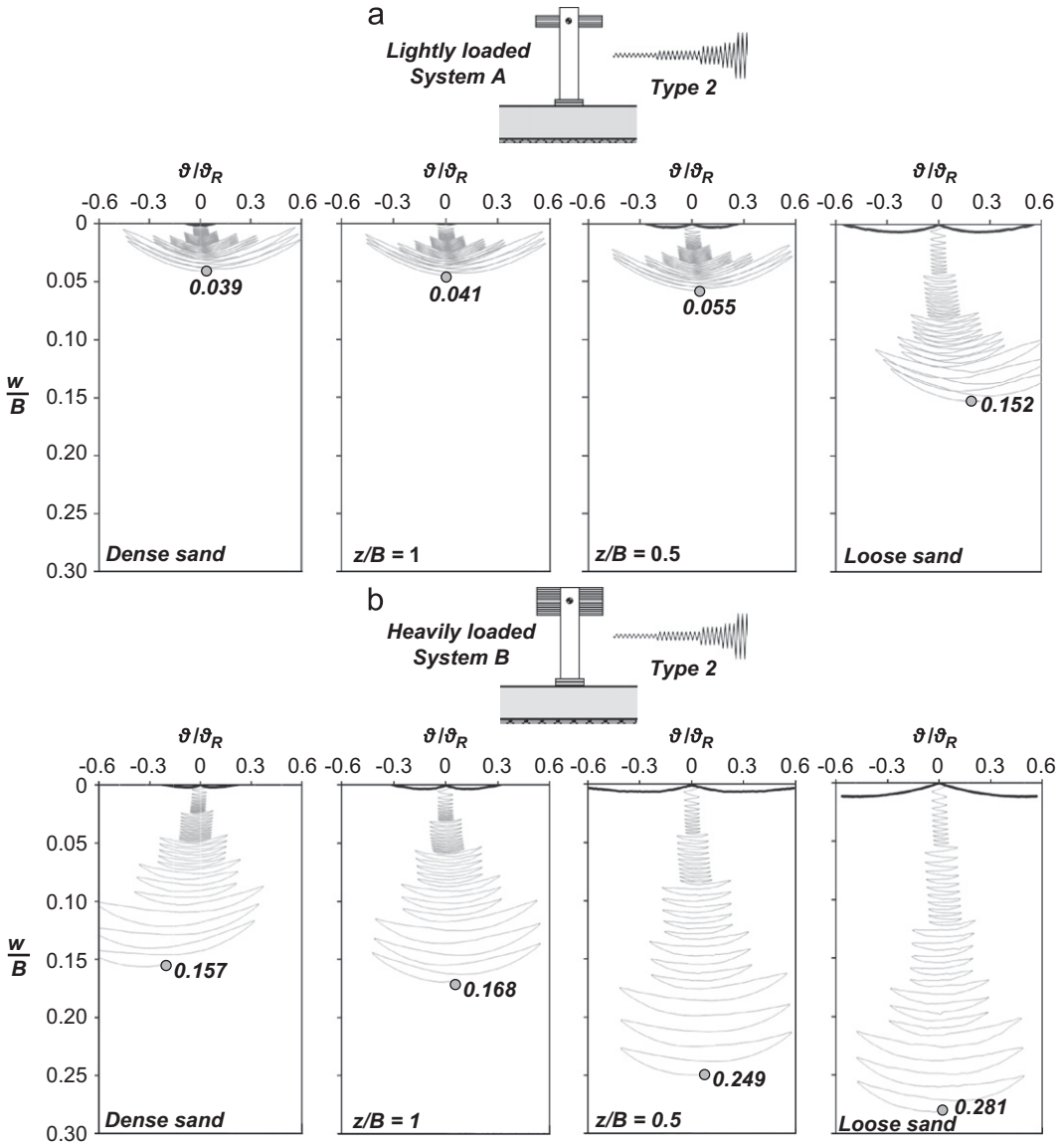

Fig. 16. Effectiveness of soil improvement for Type 2 loading protocol. Settlement–rotation response: (a) for the lightly loaded *System A*, and (b) for the heavily loaded System B ($B=0.15$ m, $\theta_R=0.167$ rad).

accumulated settlement as remarkably. The observed behavior is in accord with the previously discussed monotonic settlement–rotation response.

Not surprisingly, soil improvement is not as attractive when the same loading protocol is applied to the heavily the application of shallow-loaded *System B* (having $FS_v=5$ when founded on dense sand). As shown in Fig. 16(b), on loose sand the foundation accumulates almost two times larger settlement than *System A*. The shallow $z/B=0.5$ soil improvement is clearly insufficient as the entire loading history falls within the sinking-dominated rotation range. Interestingly, in the case of the deeper $z/B=1$ dense sand crust, although the first four loading packets fall within the sinking-dominated rotation range (which ends at $\vartheta/\vartheta_R=0.29$), a reduction in the accumulated settlement is observed and the response tends to approach that of dense sand. However, if we focus on the fifth (large-amplitude) loading packet, the performance of the $z/B=1$ improved soil is quite similar to the ideal case of the homogeneous dense sand soil profile. It is worth observing that the performance of this system founded on dense sand is quite similar to that of the lightly-loaded *System A* on loose sand, which is characterized by the same $FS_v=5$.

A more direct visualization of the performance of the two systems and the effectiveness of shallow soil improvement is offered by Fig. 17, which plots the evolution of settlement with the number of cycles for the same loading protocol. In the case of the lightly-loaded *System A* (Fig. 17(a)), the rate of settlement accumulation of the structure founded on improved soil matches the ideal case of dense sand almost right from the beginning (at $n=5$), not being noticeably affected by z/B. The performance of the $z/B=1$ soil improvement is almost identical to that of dense sand, with very slight differences being observed only at the very early stages of loading (for $n<2$). The shallower $z/B=0.5$ improvement is characterized by slightly larger settlement accumulation rate, but still its effectiveness is quite impressive. Almost the opposite is observed for the heavily-loaded *System B* (Fig. 17(b)), where the rate of settlement accumulation is substantially affected by the thickness z/B of the dense sand crust. The ideal behavior of dense sand is only approached by the deeper

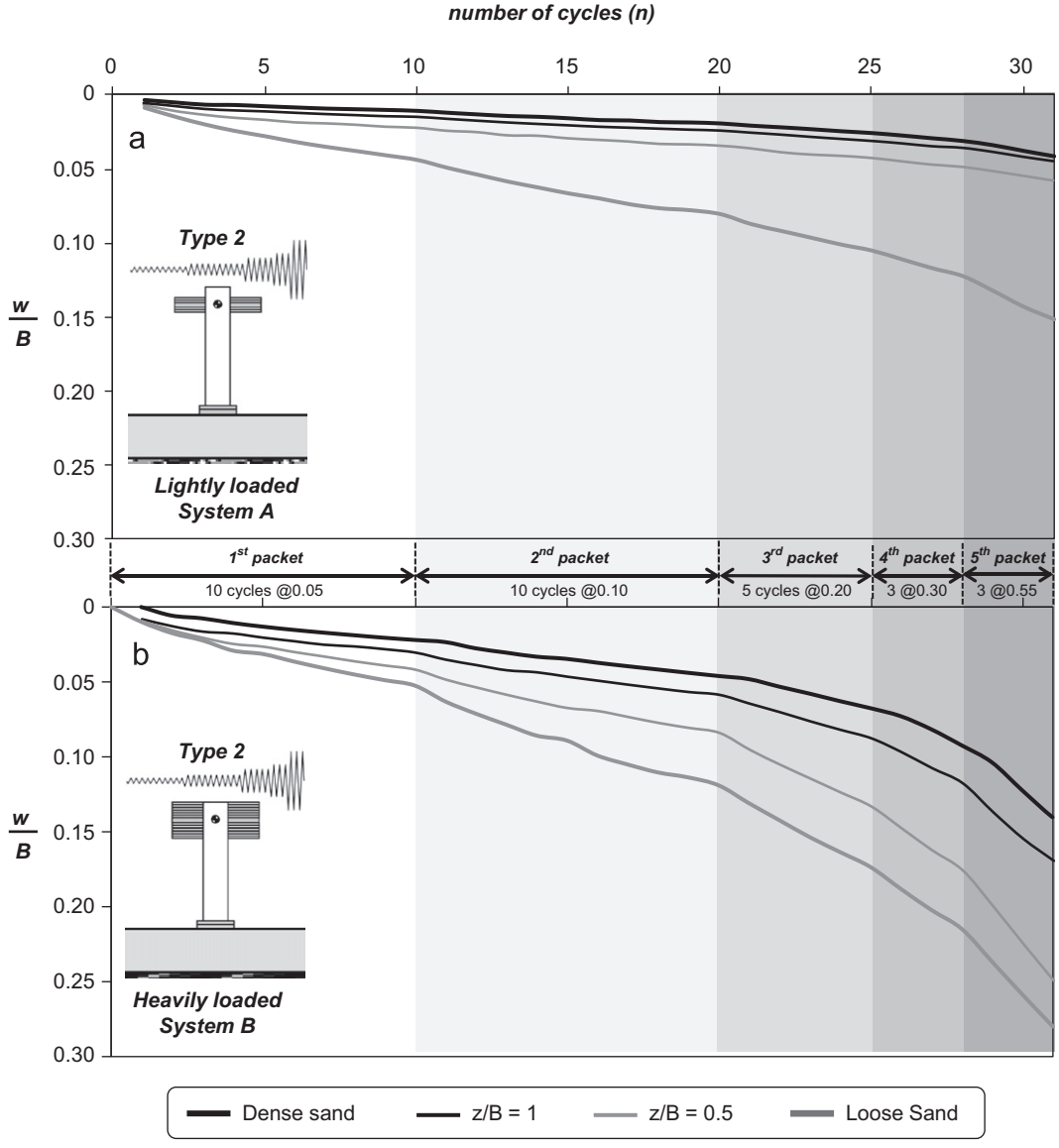

Fig. 17. Normalized settlement with respect to the number of cycles (Type 2 loading protocol): (a) for the lightly loaded *System A*, and (b) for the heavily loaded System B ($B=0.15$ m, $\theta_R=0.167$ rad).

$z/B=1$ soil improvement, but is never actually matched; differences are evident throughout the entire range of loading cycles, for all five loading packets.

7. Conclusions

This paper has investigated the rocking response of SDOF structures, and the effectiveness of shallow soil improvement stretching to various depths below the foundation. For this purpose, a series of reduced-scale monotonic and slow-cyclic pushover tests were conducted at the Laboratory of Soil Mechanics of the National Technical University of Athens. Two relatively slender $h/B=3$ SDOF systems were studied, both lying on a square foundation of width B, the first (*System A*) corresponds to a lightly-loaded structure (relatively large FS_v); the second (*System B*) refers to a heavily-loaded structure (relatively low FS_v). The two systems were used to model distinctly different foundation performance, from uplifting-dominated (*System A*) to sinking-dominated response (*System B*). The two systems were first tested on ideal and poor soil conditions (dense and medium or loose sand, respectively), to demonstrate the necessity for soil improvement. Then, the effectiveness of shallow soil improvement was studied by investigating the performance of dense sand crusts of varying depth $z/B=0.25$ to 1.

It is reminded that the conclusions of the presented research may only be applicable to relatively slender systems (bearing an h/B ratio greater than or equal to 3) where rocking response dominates over sliding. Moreover, when dealing with a frame structure the axial loads are subject to fluctuation during strong seismic shaking, and therefore FS_v will not be constant [23]. Still though, such fluctuations are not expected to alter the main findings of the presented research, which are summarized as follows:

1) When the factor of safety against vertical loads is relatively large ($FS_v > 10$ for sand), the rocking response of the foundation is mainly uplifting-dominated, not accumulating substantial settlement during sequential cycles of loading. For lower FS_V values (even of the order of 5 for sand) soil yielding takes place underneath the foundation and its response becomes sinking-dominated, leading to substantial accumulation of settlement.

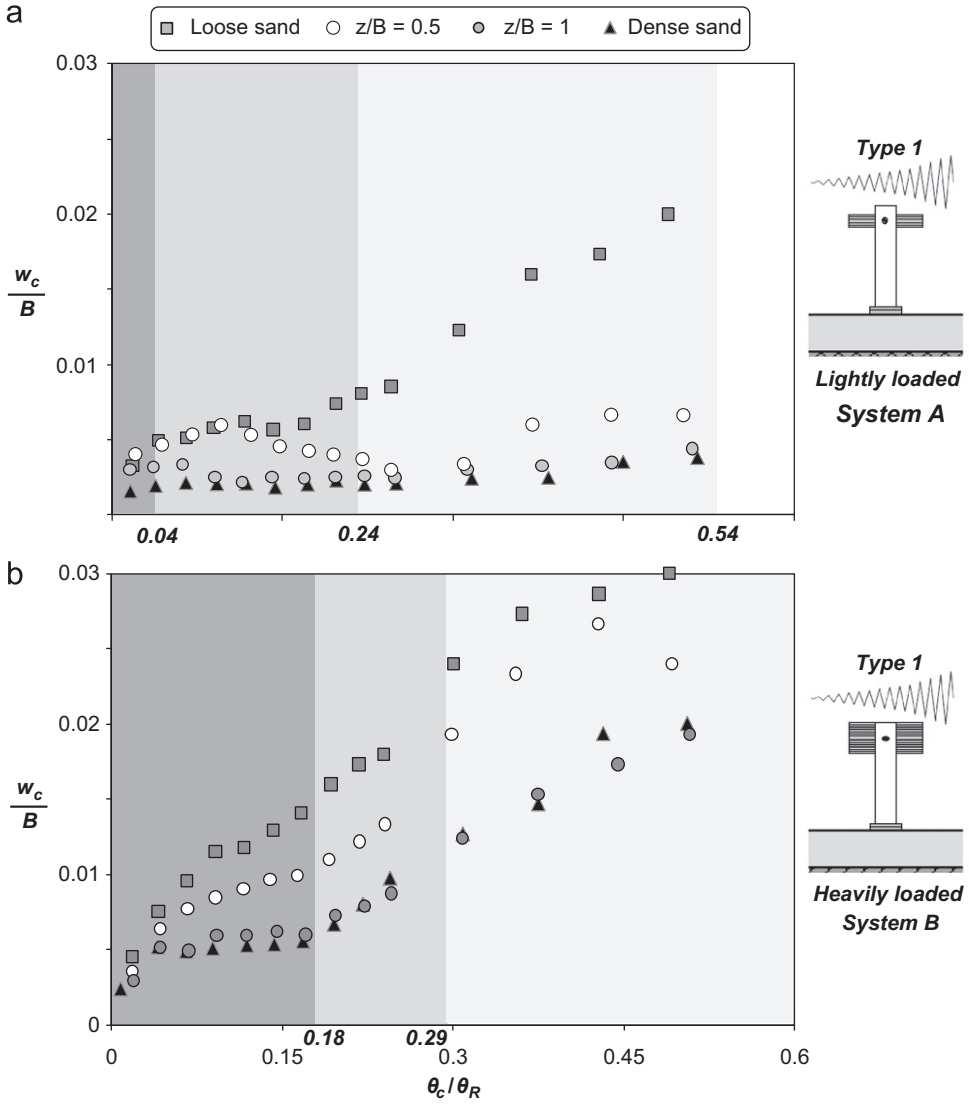

Fig. 18. Normalized settlement per cycle with respect to normalized cyclic rotation amplitude (Type 1 loading protocol): (a) for the lightly loaded *System A*, and (b) for the heavily loaded System B ($B=0.15$ m, $\theta_R=0.167$ rad). The grey-shade areas represent the rotation range for each case, in which the response is sinking-dominated (see also Figs. 9 and 12).

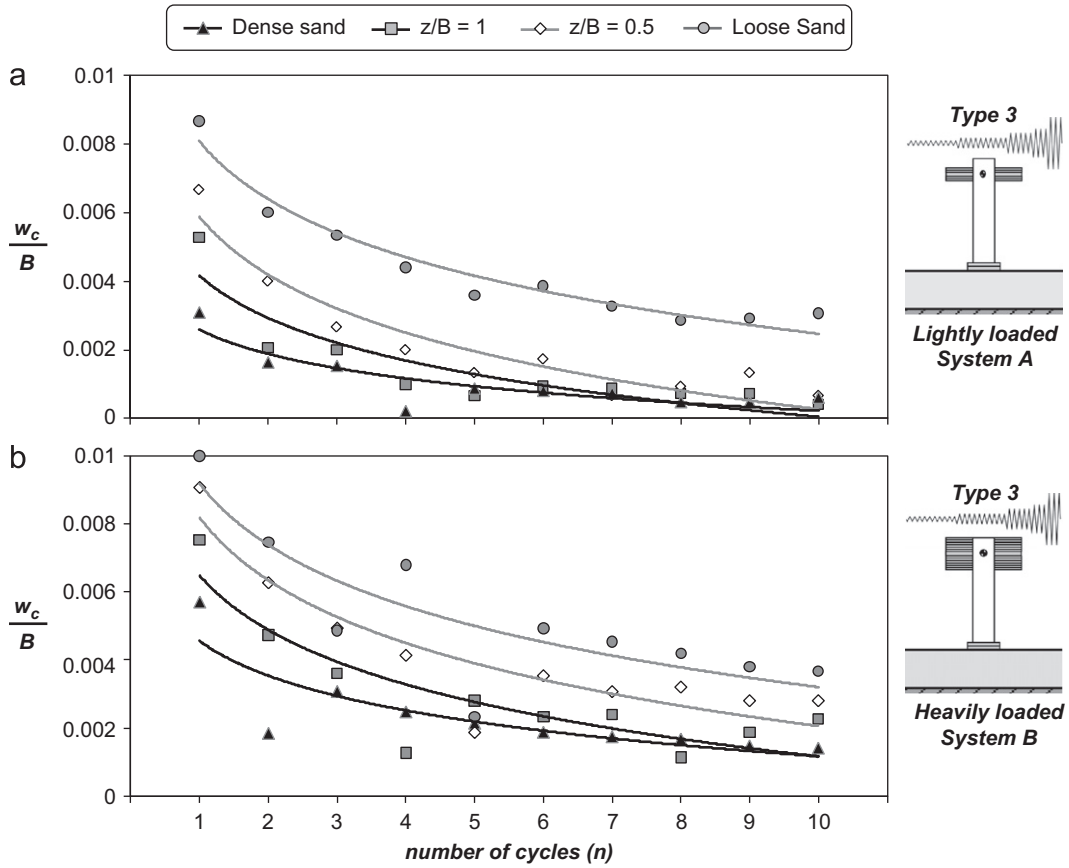

Fig. 19. Normalized settlement per cycle (Type 2 loading, 1st packet, $\vartheta=0.0167$ rad): (a) for the lightly loaded *System A*, and (b) for the heavily loaded System B ($B=0.15$ m, $\theta_R=0.167$ rad).

2) In the context of rocking isolation, foundation rocking may be desirable (to limit the inertia forces acting on the superstructure) but incorporates the peril of unacceptable settlements in case of low FS_v. Hence, in order to ensure that rocking is materialized through uplifting rather than sinking, an adequately large FS_v is required. Although this is feasible in theory, soil properties are not always well-known in reality, tending to limit the applicability of the whole concept of rocking isolation. However, since rocking-induced soil yielding is only mobilized within a shallow layer underneath the footing, "shallow soil improvement" is considered as an alternative approach to release the design from the jeopardy of an unforeseen inadequate FS_v (due to overestimation of soil properties).
3) Based on the conducted reduced-scale tests, and at least for the cases examined herein, the concept of shallow soil improvement is proven to be quite effective. A synopsis of test results is illustrated in Fig. 18, which plots the normalized settlement per loading cycle as a function of the imposed cyclic rotation amplitude for the two investigated systems. In the case of a lightly-loaded system (having $FS_v=14$ in ideal soil conditions), a $z/B=1$ dense sand crust is enough to achieve practically the same performance with the ideal case of dense sand. A shallower $z/B=0.5$ soil improvement may also be considered effective, depending on design requirements. Although results are highly dependent on nonlinearities inherent in the formation of the stress bulb, it may be conservatively concluded that an improvement layer of depth equal to the foundation width offers a safe solution for practical applications.
4) The effectiveness of shallow soil improvement is ameliorated with the increase of the cyclic rotation amplitude. As highlighted by the grey-shaded areas of Fig. 18 (which represent, for each case examined, the rotation range where the response is sinking-dominated), with the increase of soil improvement depth z/B, uplifting is promoted for a wider rotation range. For a lightly-loaded system (Fig. 18(a)), moving outside the shaded areas to larger rotations, where the response is governed by uplifting, the performance of shallow soil improvement becomes practically identical to the ideal case of dense sand. While for small θ/θ_R the foundation is in full contact with the supporting soil, generating a deeper stress bulb and hence being affected by the underlying loose sand layer, when uplifting is initiated the effective foundation width is drastically decreased, reducing the depth of the generated stress bulb. The same conclusion is practically drawn for a heavily-loaded structure (Fig. 18(b)).
5) As summarized in Fig. 19, which focuses on the evolution of normalized settlement per cycle of loading with loading cycles (as measured during the first loading packet of Type 2 protocol), the rate of settlement reduces with the increase of loading cycles. This decrease is even more pronounced in loose sand, which tends to densify with repeated cycles of loading.

Acknowledgement

The financial support for this paper has been provided under the research project "DARE", which is funded through the European Research Council's (ERC) "IDEAS" Programme, in Support of Frontier Research–Advanced Grant, under contract/number ERC-2-9-AdG228254–DARE to Professor G. Gazetas.

References

[1] Allotey N, El Naggar MH. Analytical moment-rotation curves for rigid foundations based on a Winkler model. Soil Dynamics and Earthquake Engineering 2003;23:367–81.

[2] Allotey N, El Naggar MH. An investigation into the winkler modeling of the cyclic response of rigid footings. Soil Dynamics and Earthquake Engineering 2007;28:44–57.

[3] Anastasopoulos I. Beyond conventional capacity design: towards a new design philosophy. In: Orense RP, Chouw N, Pender MJ, editors. Soil–Foundation–Structure Interaction. New York: CRC Press, Taylor & Francis Group; 2010.

[4] Anastasopoulos I, Gazetas G, Loli M, Apostolou M, Gerolymos N. Soil failure can be used for seismic protection of structures. Bulletin of Earthquake Engineering 2010;8:309–26.

[5] Anastastasopoulos I, Georgarakos P, Georgiannou V, Drosos V, Kourkoulis R. Seismic performance of Bar-Mat reinforced-soil retaining wall: shaking table testing versus numerical analysis with modified kinematic hardening constitutive model. Soil Dynamics and Earthquake Engineering 2010;30:1089–105.

[6] Anastasopoulos I, Gelagoti F, Kourkoulis R, Gazetas G. Simplified constitutive model for simulation of cyclic response of shallow foundations: validation against laboratory tests, Journal of Geotechnical and Geoenvironmetal Engineering, ASCE, in print.

[7] Bolton MD. The strength and dilatancy of sands. Géotechnique 1986;36(1): 65–78.

[8] Butterfield R, Gottardi G. A complete three-dimensional failure envelope for shallow footings on sand. Géotechnique 1994;44:181–4.

[9] Butterfield R, Gottardi G. 1995. Simplifying Transformations for the Analysis of Shallow Foundations on Sand, Proc. 5th Int. Offshore and Polar Eng Conf., The Hague, pp. 534–538.

[10] Chatzigogos CT, Pecker A, Salençon J. Macroelement modeling of shallow foundations. Soil Dynamics and Earthquake Engineering 2009;29(5):765–81.

[11] Chatzigogos CT, Figini R, Pecker A, Salençon J. A macroelement formulation for shallow foundations on cohesive and frictional soils. International Journal for Numerical and Analytical Methods in Geomechanics 2010;35:902–31.

[12] Chen XL, Lai YM. Seismic response of bridge piers on elastic-plastic Winkler foundation allowed to uplift. Journal of Sound and Vibrations 2003;266(5): 957–65.

[13] Crémer C, Pecker A, Davenne L. Cyclic macro-element for soil–structure interaction: material and geometrical nonlinearities. International Journal for Numerical and Analytical methods in Geomechanics 2001;25(12):1257–84.

[14] Drosos V, Georgarakos T, Loli M, Anastasopoulos I, Zarzouras O, Gazetas G., M. ASCE, Soil–Foundation–Structure interaction with mobilization of bearing capacity: an experimental study on Sand. Journal of Geotechnical and Geoenvironmental Engineering, ASCE, in print.

[15] Faccioli E, Paolucci R, Vivero G. 2001. Investigation of seismic soil–footing interaction by large scale cyclic tests and analytical models, Proc. 4th International Conference on Recent Advances in Geotechnical Earthquake Engineering and Soil Dynamics, Paper no. SPL-5, San Diego, California.

[16] Figini R, Paolucci R, Chatzigogos. CT. A macro-element model for non-linear soil-shallow foundation-structure interaction under seismic loads: theoretical development and experimental validation on large scale tests. Earthquake Engineering and Structural Dynamics 2011, http://dx.doi.org/10.1002/eqe.1140.2011 published online.

[17] Fukui J, Shirato M, Yoshinori N, Ryuichi A. 2005. Experimental study on the residual displacement of shallow foundations subjected to cyclic loads, Technical Memorandum of PWRI, 4027, Public Works Research Institute, Tsukuba, Japan.

[18] Gajan S, Kutter BL, Phalen JD, Hutchinson TC, Martin GR. Centrifuge modeling of load-deformation behavior of rocking shallow foundations. Soil Dynamics and Earthquake Engineering 2005;25:773–83.

[19] Gajan S, Kutter BL. Capacity, settlement, and energy dissipation of shallow footings subjected to rocking. Journal of Geotechnical and Geoenvironmental Engineering, ASCE 2008;134(8):1129–41.

[20] Gajan S, Kutter BL. Effects of moment-to-shear ratio on combined cyclic load-displacement behavior of shallow foundations from centrifuge experiments. Journal of Geotechnical and Geoenvironmental Engineering, ASCE 2009; 135(8):1044–55.

[21] Gazetas G. Analysis of machine foundation vibrations: state of the art. Soil Dynamics and Earthquake Engineering 1983;2(1):2–43.

[22] Gazetas G, Apostolou M, Anastasopoulos I. 2003. Seismic Uplifting of Foundations on Soft Soil, with Examples from Adapazari (Izmit 1999, Earthquake), BGA Int. Conf. on Found. Innov., Observations, Design & Practice, Univ. of Dundee, Scotland, Sept. 25, pp. 37–50.

[23] Gelagoti F, Kourkoulis R, Anastasopoulos I, Gazetas G Rocking isolation of frame structures founded on separate footings, Earthquake Engineering and Structural Dynamics, in print-a).

[24] Gelagoti F, Kourkoulis R, Anastasopoulos I, Gazetas G Rocking isolation of frames on isolated footings: design insights and limitations. Journal of Earthquake Engineering, in print-b.

[25] Gourvenec S. Shape effects on the capacity of rectangular footings under general loading. Géotechnique 2007;57(8):637–46.

[26] Grange S, Kotronis P, Mazars J. A macro-element for the circular foundation to simulate 3D soil-structure interaction. International Journal for Numerical and Analytical Methods in Geomechanics 2008;32:1205–27.

[27] Hardin BO, Richart FE. Elastic wave velocities in granular soils. Journal of the Soil Mechanics and Foundations Division, ASCE 1963;89(SM1):33–65.

[28] Houlsby GT, Amorosi A, Rojas E. Elastic moduli of soils dependent on pressure: a hyperelastic formulation. Géotechnique 2005;55(5):383–92.

[29] Kawashima K, Nagai T, Sakellaraki D. 2007 Rocking seismic isolation of bridges supported by spread foundations. Proc. of 2nd Japan–Greece Workshop on Seismic Design, Observation, and Retrofit of Foundations, Tokyo, Japan, pp. 254–265.

[30] Kutter BL, Martin G, Hutchinson TC, Harden C, Gajan S, Phalen JD. Status report on study of modeling of nonlinear cyclic load–deformation behavior of shallow foundations.PEER Workshop. Davis: University of California; 2003.

[31] Le Pape Y, Sieffert JP. Application of thermodynamics to the global modelling of shallow foundations on frictional material. International Journal for Numerical and Analytical Methods in Geomechanics 2001;25:1377–408.

[32] Mergos PE, Kawashima K. Rocking isolation of a typical bridge pier on spread foundation. Journal of Earthquake Engineering 2005;9(2):395–414.

[33] Muir Wood D. 2004. Geotechnical modelling. E & FN Spon (488pp) ISBN 0-419-23730-5.

[34] Nakaki DK, Hart GC. 1987 Uplifting response of structures subjected to earthquake motions, Report No. 2.1-3, U.S.–Japan Coordinated Program for Masonry Building Research.

[35] Negro P, Paolucci R, Pedretti S, Faccioli E. 2000. Large-scale soil–structure interaction experiments on sand under cyclic loading, Proceedings of the 12th World Conference on Earthquake Engineering, Auckland, NewZealand, 2000, paper 1191.

[36] Nova R, Montrasio L. Settlement of shallow foundations on sand. Geotechnique 1991;41(2):243–56.

[37] Panagiotidou AI, Gazetas G, Gerolymos N. Pushover and seismic response of foundations on stiff clay: analysis with P-Δ effects, Earthquake Spectra, in print.

[38] Paolucci R. Simplified evaluation of earthquake-induced permanent displacements of shallow foundations. Journal of Earthquake Engineering 1997;1(3): 563–79.

[39] Paolucci R, Shirato M, Yilmaz MT. Seismic behaviour of shallow foundations: shaking table experiments vs numerical modeling. Earthquake Engineering and Structural Dynamics 2008;37:577–95.

[40] Pecker A. 1998. Capacity design principles for shallow foundations in seismic areas. Proc. 11th European Conference on Earthquake Engineering, A.A. Balkema Publishing.

[41] Pecker A. 2003. A seismic foundation design process, lessons learned from two major projects: the Vasco de Gama and the Rion Antirion bridges, ACI International Conference on Seismic Bridge Design and Retrofit, University of California at San Diego, La Jolla, USA.

[42] Pedretti S. 1998. Non-linear seismic soil-foundation interaction: analysis and modeling methods, PhD Thesis, Politechnico di Milano.

[43] Priestley MJN, Seible F, Calvi GM. Seismic Design and Retrofit of Bridges. New York: John Wiley and Sons; 1996.

[44] Raychowdhury P, Hutchinson TC. Performance evaluation of a nonlinear Winkler-based shallow foundation model using centrifuge test results. Earthquake Engineering and Structural Dynamics 2009;38:679–98.

[45] Seed HB, Wong RT, Idriss IM, Tokimatsu K. Moduli and damping factors for dynamic analyses of cohesionless soils. Journal of Geotechnical Engineering, ASCE 1986;112(11):1016–32.

[46] Shirato M, Kouno T, Asai R, Nakani N, Fukui J, Paolucci R. Large-scale experiments on nonlinear behavior of shallow foundations subjected to strong earthquakes. Soils and Foundations 2008;48(5):673–92.

[47] Taiebat HA, Carter JP. Numerical studies of the bearing capacity of shallow foundations on cohesive soil subjected to combined loading. Géotechnique 2000;50(4):409–18.

[48] Tan FS 1990. Centrifuge and theoretical modelling of conical footings on sand, Ph.D. Thesis, University of Cambridge.

[49] Yim SC, Chopra AK. Simplified earthquake analysis of structures with foundation uplift. Journal of Structural Engineering (ASCE) 1985;111(4): 906–930.